

**A New Generation of Selective Androgen Receptor Degraders: Our Initial Design,
Synthesis, and Biological Evaluation of New Compounds with Enzalutamide-Resistant
Prostate Cancer Activity**

*Dong-Jin Hwang,[†] Yali He,[†] Suriyan Ponnusamy,[‡] Michael L. Mohler,^{†,#} Thirumagal
Thiyagarajan,[‡] Iain J. McEwan,[&] Ramesh Narayanan,[‡] Duane D. Miller^{*,†}*

[†]. Department of Pharmaceutical Sciences, University of Tennessee Health Science Center,
Memphis, TN 38163.

[‡]. Department of Medicine, University of Tennessee Health Science Center, Memphis, TN
38103.

#. GTx, Inc., Memphis, TN 38103.

&. School of Medicine, Medical Sciences and Nutrition, Institute of Medical Sciences,
University of Aberdeen, Aberdeen AB25 2ZD, Scotland, UK

ABSTRACT: In our effort to find small molecule treatments of advanced prostate cancers (PCs), the novel series of indolyl and indolinyl propanamides (series **II** and **III**) were discovered as selective androgen receptor degraders (SARDs). Initial studies of androgen receptor (AR) antagonist (**1**) and agonist (**2**) propanamides yielded a tertiary aniline (**3**) with novel SARD activity but poor metabolic stability. Cyclization to **II** and **III** produced sub-micromolar AR antagonism and protein degradation selective to AR and AR splice variant (AR SV). **II** and **III** maintained potency against enzalutamide-resistant (Enz-R) mutant ARs and PC cells, and were efficacious in Enz-R xenografts, suggesting their potential to treat advanced PCs. Disclosed is the design, synthesis, and biological activity of novel SARDs that could potentially be used for the treatment of a wide spectrum of PCs including castration resistant, Enz-R, and/or AR SV dependent advanced PCs that are often untreatable with known hormone therapies.

KEYWORDS: Structure-activity relationship, Selective androgen receptor degrader, Androgen receptor, Androgen receptor splice variant, AR-V7, AR escape mutants, Antagonist, Prostate cancer, Antiandrogen resistance, Enzalutamide resistance, Castration-resistant prostate cancer, N-terminal domain, Ligand binding domain, Prostate-specific antigen, AR activation function domain-1.

1. INTRODUCTION

The androgen receptor (AR) has been the focus of prostate cancer (PC) therapies since Huggins and Hodges's discovery in the early 1940s that androgens promote PC growth.¹⁻³ PC is one of the most common malignancies diagnosed in men. According to the American Cancer Society in 2017, 161,000 men were diagnosed with PC in the United States with 26,730 deaths

estimated from the disease.⁴ More than 3 million men in the United States are currently living with PC.⁵ The AR plays an important role not only for the development and function of the normal prostate gland, but also for the growth and maintenance of PC cells.⁶⁻⁷ Androgen deprivation therapy (ADT), via suppression of endogenous synthesis (e.g., goserelin or abiraterone) and/or AR blockade (e.g., bicalutamide (**4**), enzalutamide (**5**), and apalutamide (**6**) in Figure 1), is the standard of care for metastatic PC. Re-activation of the AR-axis despite treatment can occur even despite castration levels of testosterone or 5 α -dihydrotestosterone (DHT), suggesting the need for new mechanisms for AR antagonism.⁸⁻¹⁰

An AR antagonist **5** improved survival of men with metastatic castration-resistant prostate cancer (CRPC).¹¹ Earlier this year, the AR antagonist **6** was approved for use in non-metastatic CRPC based on its ability to extend the metastasis-free survival as compared to placebo.¹²⁻¹³ Unfortunately, primary and acquired resistance to **5** (and other antiandrogens) is common,¹⁴⁻¹⁵ e.g., the mutations AR F876L or F876L-T877A switch **5**, at higher levels, from AR antagonist to agonist making PCs enzalutamide-resistant (Enz-R).¹⁴ Further, cross-resistance between **5** and **6** based on F876L¹⁶ and cross-resistance in general between abiraterone and/or ligand binding domain (LBD)-directed antiandrogens is well known.¹⁷⁻¹⁹ Moreover, AR splice variants (e.g., AR-V7 and D567es) lacking the LBD have been reported as pan-resistant CRPCs.¹⁹ The development of resistance to antiandrogens is a growing concern and new strategies to block AR function in CRPC are required.¹⁷⁻¹⁹

Our first generation of selective androgen receptor degraders (SARDs) were metabolically labile secondary and tertiary amines (**I**) lacking *in vivo* activity when administered orally that were designed by structural modification of the AR antagonist **1** [2-hydroxy-4-(4-isothiocyanatophenyl)-2-methyl-N-(4-nitro-3-(trifluoromethyl)phenyl)butanamide] and the

tissue-selective AR agonist enobosarm (**2**, (*S*)-*N*-(4-cyano-3-(trifluoromethyl)phenyl)-3-(4-cyanophenoxy)-2-hydroxy-2-methylpropanamide) (Figure 2). Class **I** was exemplified by UT-69 (**3**, (*S*)-*N*-(4-cyano-3-(trifluoromethyl)phenyl)-3-((6-cyano-[1,1'-biphenyl]-3-yl)(methyl)amino)-2-hydroxy-2-methylpropanamide) whose tertiary amine was cyclized to form indoles (**II**) and indolines (**III**), which are characterized herein as potent AR antagonists and SARDs with a broad activity profile in models of prostate cancer, and *in vivo* AR antagonism when orally administered. E.g., SARDs of **II** and **III** exhibited strong AR antagonistic activity *in vitro* in transcriptional activation and cellular proliferative assays, including in models of enzalutamide-sensitive and Enz-R PCs, and CRPCs. Additionally, **II** and **III** showed selective AR degradation of full-length (FL; e.g., from LNCaP cells (T877A)) and splice variant (SV; e.g., from 22RV1 cells (AR-V7)) isoforms of AR, all at sub to low micromolar treatment levels, and in a variety of PC cell contexts, including Enz-R PCs (e.g., MR49F cells).

The ability to degrade SV AR in this study suggested the potential of **II** and **III** to treat various currently untreatable advanced and refractory PCs. E.g., those lacking the ligand binding domain (LBD) of AR such as AR-V7 and D567es AR truncations, which are not susceptible to ADT, abiraterone, or LBD-directed antiandrogens (e.g., **4-6** (Figure 1)), and are associated with short survival.²⁰⁻²¹ Further, *in vivo* investigations found that analogs within the **II** and **III** series overcome a variety of escape mutants including F876L and F876L/T877A that are known to emerge due to treatment with **5**. These mutations convert **5** and **6** to agonists, conferring resistance to prostate cancer cells and tumors²² via an agonist switch as seen with other LBD-binding antiandrogens, e.g. W741L for **4** and T877A for flutamide (*N*-(4-nitro-3-(trifluoromethyl)phenyl)isobutyramide).²³⁻²⁴

The intractability of truncation mutants and the frequency of the agonist switch mutations suggest that novel ways, potentially LBD-independent ways, of targeting the AR are needed. The initial design, synthesis and biological evaluation of these SARDs as putative treatments of Enz-R and other advanced PCs is discussed. Moreover, these SARDs are dual acting agents, i.e., potent inhibitors and degraders of AR, providing a higher evolutionary barrier to the development of resistance to **II** and **III**. For all these reasons, we believe that SARDs may provide a next generation of AR antagonists to treat a variety of refractory and/or advanced PCs, including Enz-R and AR-V7 dependent PCs.

Herein we rationalize our profile of screening assays designed to overcome Enz-R PC including our initial SARD structure activity relationship (SAR). Further, **II-III** were evaluated in *in vitro* anti-proliferation and *in vivo* xenograft models of Enz-R PC. In overview, we report three series of SARDs (**I-III**) possessing a novel mechanism of action in SV AR and escape mutant models of Enz-R PC *in vitro* and *in vivo* assays. Despite a variety of competing preclinical approaches to address Enz-R, there has been little success in the clinic, leaving this and other refractory prostate cancers as unmet clinical needs. It is our belief that the SARDs such as reported herein may resurrect the AR axis as a target for overcoming Enz-R, AR-V7 dependent, and/or refractory CRPCs.

2. RESULTS

Design. Since even before our discovery of diaryl nonsteroidal androgens in 1998,²⁵⁻²⁷ we have designed and developed many variations of AR agonist and AR antagonist propanamides with a recent focus on selective androgen receptor degraders (SARDs or AR degraders; where selectivity refers to degrading only the AR protein) such as **3** and **7** (Figures 1 and 2).²⁸ SAR studies of the propanamides demonstrated that the linkage to the B-ring plays a

key role in determining the agonistic *vs.* antagonistic activities (Figure 2), which can be fine-tuned via B-ring substitution.^{25-27, 29-40} Many ethers (and thioethers *in vitro*) are agonists whereas most other linkages are partial to full antagonist. E.g., enobosarm (ostarine, MK-2866, GTx-024, S-22, **2** in Figure 1) showed strong *in vivo*^{36, 40-42} tissue-selective androgen receptor modulation (SARM) activity. In other words anabolic tissue-selectivity is revealed by increased lean body mass reflective of muscle mass changes, increased bone mineral density and performance enhancement in humans across at least 22 clinical trials.^{43,44}

We also have reported high affinity *p*-NCS B-ring substituted propanamides with a variety of linkages to the B-ring such as methylene (e.g., **1** which is a butanamide), secondary and tertiary amine, ether, thioether, and sulfone propanamides.²⁷ Though compounds like **1** were designed as antagonists that irreversibly bind the AR via the NCS moiety, we were only able to demonstrate moderate (μM) anti-proliferation in prostate cancer cell lines (IC_{50} values of 20.6-23.8 μM in various PC cell lines). Seeking to improve the efficacy in models of PC, we explored the B-ring substitution in a series of secondary and tertiary amines (i.e., class **I** SARDs). The high inhibitory potency of the amines led to the discovery of **3** (Figure 2) and its characterization as our initial SARD providing an entry into AR degradation and helping to define the structural characteristics of propanamide SARDs.²⁸ Fusion of the tertiary amine of **3** into the B-ring retained both the AR inhibition and SARD activities at very high potency but with improved ligand efficiency and *in vitro* stability, as exemplified by the indole **7** in Figure 1.²⁸ Further, **3** and **7** did not degrade glucocorticoid receptor (GR), estrogen receptor (ER), or progesterone receptor (PR) expressed in cells, demonstrating the AR selectivity of **I-III**.²⁸ The ability to degrade AR was generalizable to a series of N-linked indoles (**II**), indolines (**III**) (Figure 2), and various other bicyclic heterocycles (not reported here).

Our initial [or seminal] SARD SAR exploration is detailed herein. Further, class **II-III** SARDs in Figure 2 are evaluated for *in vitro* anti-proliferation and anti-xenograft activities in models of Enz-R PC. Unlike previous antiandrogens lacking SARD activity such as **4** and **5**, **I-III** have the potential to overcome all AR-dependent PC models tested to date, including Enz-R and/or SV AR expressing CRPCs.

Initial Biological Evaluation of Class I. Herein, we have sought to design new molecules to potently inhibit and degrade AR with the specific aim to treat CRPC. Initially, we tested a couple of high affinity but weakly antiproliferative butanamides (i.e., methylene-linked propanamides) such as **1** and **8** for AR antagonistic activity and their ability to degrade AR at the protein level as shown in Table 1. SARD activity reported as percent degradation captures the AR protein levels relative to vehicle treated and are reported qualitatively using the following abbreviations: -, no degradation (inactive); +, < 30% degradation (weak SARD activity); ++, 31 ~ 60% degradation (moderate SARD activity); +++, 61 ~ 90% degradation (strong SARD activity); +++++: > 90% degradation (complete SARD activity). [The terms inactive, weak, moderate, strong and complete AR degradation and the symbols are used interchangeably.] High affinity **1** (0.032 μM)²⁷ did not inhibit AR transactivation *in vitro* (> 10 μM) despite weak (SV) to moderate (FL) SARD activity; whereas non-binder **8** showed sub-micro molar level *in vitro* inhibition (0.392 μM) and moderate FL SARD activity.

Though interesting, these activity profiles did not provide potent inhibition and FL AR and SV AR degradation in a single molecule, nor consistent antagonism. However, changing the methylene linkage to amine provided a series of compounds with the *in vitro* profile we were looking for, the ability to potently inhibit and degrade FL and SV AR (Table 1). Biaryl B-ring **3** emerged as the lead molecule from series **I**, demonstrating highly potent inhibition *in vitro* (48

nM) and strong SARD activity that almost completely degrades FL and SV AR at sub- μ M and low μ M levels, respectively (Table 1).²⁸ The shifted nitrogen atom illustrated in Figure 2 produced a unique biological action with the potential to overcome CRPC whether based on AR point mutation or AR truncation. However, the biphenyl B-ring and methyl substituent of the amine proved to be metabolic liabilities, limiting the bioavailability of **3**, making observation of AR antagonism *in vivo* inaccessible.²⁸ These metabolic liabilities were removed by cyclization of **3** to form classes **II** (indole) and **III** (indoline) SARDs possessing a nitrogenous heterobicyclic B-ring (Figure 2) which did not require aryl substitution and provided new Lipinski-compliant⁴⁵ chemotypes (Table 2) to co-optimize for antagonism, SARD activity (*infra*), and drug metabolism and pharmacokinetic (DMPK) properties (*infra*), with emphasis on SARD efficacy.

We synthesized the indolyl **II** and indoliny **III** classes of new derivatives and evaluated the SAR of the SARD activities of these compounds. The A-ring was conserved except for two variants at the 3'-position, namely 3'-CF₃ and 3'-Cl anilides (Table 2). In overview, **II-III** maintained the high efficacy degradation of FL AR at 1 μ M dose and SV AR at 10 μ M dose, and high potency antagonism (two digit nano-molar range) of **3**. Unlike the previous nonsteroidal AR agonists or antagonists including **4-6** and abiraterone, the structurally optimized members of **II-III** showed AR antagonism in *in vivo* models including models of CRPC.

Synthesis. Compounds **1** and **8** previously reported by our group²⁷, are representative examples of a series of carbon-linked AR antagonists and were synthesized as previously reported. **2**, an ether linked agonist, was also synthesized as previously reported for other ether linked propanamides.^{29, 46} **1** and **2** each have a nitrogenous substituent on the aromatic B-rings. In **1** the nitrogen atom in the isothiocyanate group is α to the B-ring whereas **2** has a β nitrogen atom in the cyanide group (Figure 2).

In our design, we shifted the nitrogen into the linkage to produce multiple series (**I-III**) with a common unique biological profile which is optimally represented as **3** and **7**. **3** was synthesized as previously reported (see supplementary section).²⁸ The present study illustrates a series of indolyl (**II**) and indolinyl (**III**) small molecule SARDs which were designed and synthesized as diaryl (*S*)-propanamides with two variations of the anilide ring, 3'-CF₃ and 3'-Cl anilides. SAR studies of **II-III** focused on substitution of the B-ring. The synthesis of **II** and **III** is outlined in Scheme 1. We prepared both the class **II** and **III** starting from a chiral hydroxyl bromide **11** (Scheme 1) reacted with an aniline (**9** or **10**) to form an *R*-bromoaniline (**12** or **13**), followed by oxirane (**14** or **15**) formation in the presence of K₂CO₃ (or other basic conditions), via a known procedure.^{27, 37, 47-48} In overview, compounds of **II** were prepared in very good yield by Method A via activation of substituted-1*H*-indoles (**16**) with sodium hydride and, its subsequent reaction with the oxiranes **14** or **15**. Similarly, compounds of **III** were prepared by Method B which uses LDA to activate substituted 1*H*-indolines (**17**) to react with the same oxiranes (**14** or **15**), as depicted in Scheme 1. Indoline **21f** was prepared by reduction of indole **19f** as described in the Experimental Section. Although most compounds **16** and **17** were commercially available, indoles **16a-c** were *de novo* synthesized in our lab as described in the Experimental Section.

The *R*-bromoanilides **12** and **13** were synthesized as enantiomerically pure products via the conserved intermediate bromo-acid **11** (*R*-isomer) which was synthesized in large quantities from *D*-proline as the chiral auxiliary, as previously reported.^{27, 49} Final products were diaryl (*S*)-propanamides. To further probe the SAR, the opposite isomer of **7**, namely **7r** was prepared from the *S*-isomer of compound **11** derived from *L*-proline via the same synthetic method to yield an (*R*)-propanamide.

Overview of the Biological Evaluation of Class II and III SARDs. SAR-guided substitution of the B-ring allowed co-optimization of AR antagonism and AR degradation activities for the treatment of Enz-R or SV AR expressing CPRC. The screening regimen included determination of AR LBD binding affinity, inhibition of R1881-activity *in vitro* transcriptional activation (sometimes stated as *in vitro* antagonism herein), and degradation of FL and SV ARs, as shown in Tables 1, 3 and 4. Once potent full antagonism and strong pan-SARD activity were accomplished in a single molecule, DMPK criteria (e.g., see *in vitro* liver microsome stabilities studies reported *infra*) were also considered in the selection of SARDs to be tested for *in vivo* efficacy.

***In vitro* screening: AR LBD binding (K_i), wild type antagonism (IC_{50}), and FL and SV SARD activity (% degradation).** In separate batches of the stated *in vitro* assays, **7** (5-F indole)²⁸ was included as a positive control, so that variations in the assays could be recognized. The desired screening profile consisted of: (1) strong (+++) or complete (++++) efficacy FL AR degradation in LNCaP cells possessing T877A (recently reported as T878A with all other amino acid numbers also shifted by +1, whereas traditionally numbered as T877A) mutant AR conferring resistance to hydroxyflutamide, (2) strong (+++) or complete (++++) efficacy SV AR degradation in 22RV1 cells possessing AR-V7 truncation mutant AR, which is theoretically resistant to all LBD-targeted antiandrogens, and (3) at least mid nanomolar (nM) potency *in vitro* antagonism to block any residual wildtype or mutant AR that might be present despite strong to complete degradation. (Binding affinity to purified LBD AR was determined but was not used to select leads, as discussed in the next section.)

Following screening, promising compounds were tested in DMPK assays, e.g., the mouse liver microsome (MLM) assay reported *infra*, to determine their relative stability and/or to locate

their metabolic liabilities such that they can be blocked. This allows us to advance only relatively stable compounds possessing all three screening criteria to *in vivo* testing, including in models of CPRC.

LBD vs. Activation Function-1 (AF-1) Binding and Antagonism. Equilibrium-binding affinity (K_i) of series **II** and **III** was measured using binding to purified GST-tagged human AR LBD in competition with a non-metabolizable and stable steroidal androgen, [^3H]-mibolerone ([^3H]MIB) (at 1 nM). The specific binding at each concentration of the test compounds was obtained by subtracting the non-specific binding of [^3H]MIB, and the values are expressed as the percentage of the specific binding in the absence of the compound of interest.

All assay batches were normalized to the respective K_i value for DHT in each assay, which was considered as 1 nM. The concentration of compounds **II** or **III** that reduced the specific binding of a radiolabeled [^3H]MIB by 50% (IC_{50}) was determined by computer fitting the data to the following equation using SigmaPlot[®] and four parameter logistics.

We hypothesized that series **I-III** will need to make at least a transient interaction with AR to enable its ubiquitination-dependent degradation,²⁸ suggesting the importance of AR binding. However, when we tested the degradation properties of **II** and **III**, these values correlated poorly with the AR LBD affinity assay described herein (Tables 3 and 4). Better correlation was seen between the level of degradation in LNCaP and 22RV1 cells and AR antagonism. Further, the series **II** and **III** exhibited antiproliferative activity in Enz-R cells (see MR49F⁵⁰ data *infra*) suggestive of phenotypic effects resulting from the antagonism and SARD activities reported here. Though generalization is difficult, SARDs of series **II** and **III** produced hit or miss nM level binding (ranged from 0.047 to >10 μM) and more consistently potent AR antagonism (ranged from 0.026 μM to 0.835 μM). Regarding selectivity of antagonism, equipotent PR antagonism was

observed for **7**²⁸ and selected members of **II** and **III** (data not shown), but not other steroid hormone receptors. E.g., indoles **19f** and **19b** and indolines **21a** and **21b** lack significant GR antagonism in *in vitro* transactivation studies, as shown in Supplementary Figure S1. Further, **19f** and **19b** also lack the ability to antagonize the ER *in vitro*. Given the lack of antagonism of GR or ER with the above and other SARDs, we do not routinely screen for GR and ER degradation.

The poor correlation between AR LBD binding and antagonist or SARD activity is clearly seen for the optical isomers **7** and **7r**.²⁸ They demonstrated comparably high efficacy SARD activities despite their disparity in binding affinities (0.267 μ M (**7**) vs. >10 μ M (**7r**)). We have previously addressed possible rationalizations of this behavior, which include the N-terminal domain (NTD) binding site for our SARDs reported for **7**, **7r**, and **3** which differentiates our compounds from other SARDs or proteolysis-targeting chimaeras (PROTACs).²⁸

Several lines of biophysical evidence substantiate that AF-1 binding is generalizable for **I-III**, including fluorescence polarization for **19b** (Supplemental Figure S2) and previously for **3**²⁸ and **7**²⁸, and previous NMR studies for **7**²⁸ and **7r**²⁸, as well as these and other biophysical methods applied to these and other structural classes of SARDs not reported here (unpublished results). The fluorescence polarization study with **19b** demonstrated an interaction of the SARD with AF-1 domain. The interaction was revealed as a shift in the fluorescence emitted by the tyrosine and tryptophan residues in the presence of **19b**, which is consistent with the aforementioned previous results. The AF-1 domain is present in the N-terminus of the AR and is common to all forms of the AR expressed in cells. We believe AF-1 binding to be a general mechanism of action for our SARDs but do not routinely screen new compounds biophysically.

Moreover, our SARDs may induce degradation by perturbing AR folding or modulating the protein-protein interactions of AR. These would not necessarily be reflected in AR LBD binding affinities.

The previous notwithstanding, the AR LBD affinity (for most compounds) and *in vitro* antagonist properties of **II** and **III** ranged from comparable to favorable relative to the standard known AR antagonists currently employed clinically for the treatment of PC. E.g., **4**, **5**, and **6** had binding affinities of 0.509 μM , 3.641 μM , and 1.452 μM , and *in vitro* antagonism of 0.248 μM , 0.216 μM , and 0.016 μM (the last value was previously reported⁵¹), respectively, compared to **7** binding of 0.267 μM and antagonism of 0.085 μM . Despite the standard agents being potent antagonists, only **6** demonstrated any SARD activity albeit with lower efficacy (<30%), as shown in Table 3. As expected and consistent with steroidal AR agonists, the nonsteroidal SARM **2** stimulated expression of FL and SV AR as seen by Western blot, affirming that AR protein levels in the SARD assay behaved as expected. In contrast, the series **II** and **III** degraded FL AR at 1 μM dose and also SV AR at 10 μM (22RV1) with efficacies ranging from 30-100%. In some cases, the reduction of AR protein levels was nearly 100% and occurred at nM levels (*infra*). Our current view is that the SARD activity of these compounds is of primary importance to their ability to overcome CRPC. Consequently the SAR discussion below will focus on SARD activity.

Our SARDs display a novel mechanism of action, which, by its nature, provides a rationale for an expanded disease scope of efficacy and a barrier to the development of mutational resistance.²⁸ Below, AR antagonism will only be discussed as a secondary consideration in the biological evaluation.

SARD assays in LNCaP and 22RV1 cell lines. We screened all compounds of **II** and **III** for their ability to degrade FL (LNCaP) and SV (22RV1) androgen receptors (Tables 1, 3 and 4). Western blots for representative compounds from **II** and **III** are shown in Figure 3. SARD activity was measured by treating cells with several doses, e.g., 0.1, 1.0 and/or 10 μ M, of SARDs in the presence of agonist (0.1 nM R1881). LNCaP or 22RV1 cells were plated in full serum containing medium. Medium was replaced with 1% charcoal-stripped fetal bovine serum (csFBS) containing medium and the cells were maintained in this medium for 2 days. Medium was changed again after 2 days and the cells were treated as indicated in the figures in the presence of 0.1 nM R1881. Cells were harvested 24 h after treatment and Western blot for AR and actin was performed using specific antibodies.

The Western blots were quantified densitometrically and the AR/actin values are represented as fold change or percent change from vehicle-treated cells. Panel A in Figure 3 showed the degradation of FL AR in LNCaP cells and Panel B showed degradation of SV AR in 22RV1 cells, while actin in each lane serves as an internal standard to correct for variations in protein loading which complicate the visual interpretation of the immunoblots. The percent (%) degradation values reported in Tables 1, 3, and 4 are normalized for variations in protein loading and are relied upon for relative efficacy determinations. Dose-dependent degradation was seen in LNCaP cells for **21f** (3'-Cl, 5-F, 6-Ph indoline), **19f** (3'-Cl, 5-F, 6-Ph indole), **19b** (3'-Cl, 4-F indole), **20b** (3'-CF₃, 4-F indoline), **21b** (3'-Cl, 5-F indoline) and **21d** (3'-Cl, 6-F indoline). From Figure 3A, it is apparent that >50% of FL AR is already degraded at 1 μ M of these SARDs, i.e. nM range SARD activity. SV AR degradation (the lower molecular weight band in Figure 3B; upper band is disregarded in % degradation values) for the selected SARDs **21f** (3'-Cl, 5-F, 6-Ph indoline), **19f** (3'-Cl, 5-F, 6-Ph indole), **21a** (3'-Cl, 4-F indoline), and **7** (3'-CF₃, 5-

F indole) was observed to be dose-dependent and generally about 10-fold less potent (Figure 3B) than FL AR degradation, which is consistent with our other SARDs. Some compounds degrade FL AR better than SV AR (e.g., **21d**) or vice versa (e.g., **18f**) (Tables 3 and 4), whereas the optimal SARD will potently and completely (i.e., +++) degrade both and has a high potency antagonism. **21f** comes closest to displaying the perfect profile with complete/strong degradation of FL/SV and antagonism comparable to **5**, 0.244 μM (**21f**) vs. 0.216 μM (**5**), but weaker than other SARDs reported here.

Selectivity and mechanistic aspects of SARD activity: The AR selectivity of degradation among steroidal receptors has been shown previously, e.g. **3** and **7** were shown to not degrade the expression of PR, ER, and GR²⁸. Supplemental Figure S3 further supports this view as it demonstrates that **19b** and **19f** do not degrade ER in MCF-7 cells. Moreover, the absence of significant antagonism of GR by **19b**, **19f**, **21a** and **21b** nor ER antagonism by **19b** and **19f** (Figure S1 discussed *supra*) further supports the lack of degradation of these receptors. Although LBD binding may not correlate to degradation, steroidal receptor antagonism would be expected if that steroid receptor is degraded.

To validate that SARDs function by reducing the stability of protein (as opposed to decreasing rate of protein synthesis, e.g., lowering mRNA levels, etc.), we conducted an experiment with **19f** in the presence of the general protein synthesis inhibitor, cycloheximide (Supplemental Figure S4). Treatment of LNCaP cells with 50 μM cycloheximide or 10 μM **19f** did not significantly reduce the protein levels at the evaluated time-points. However, when the cells were treated with the two molecules together, significant down-regulation of the AR was observed. These results suggest that the SARDs function by destabilizing the AR protein that has already been synthesized as opposing inhibiting protein synthesis. This agrees well with an

earlier validation of **3** and **7** using very similar methodology.²⁸ Further, **7** was previously characterized as increasing rate of AR degradation by targeting AR to the proteasome in LNCaP cells using bortezomib.²⁸ That result was confirmed for indoles reported first herein using the same methodology but in an EnzR LNCaP cell line (see *infra*), suggesting that proteosomal degradation of AR can overcome EnzR.

SARD SAR. As described above, two classes of SARDs were prepared, **II** (indoles) and **III** (indolines), as either 3'-CF₃ (**18** and **20** series) or 3'-Cl (**19** and **21** series) anilines as shown in Table 2. The B-rings of **II** and **III** were substituted with a variety of electron withdrawing (e.g., halogens, nitro, trifluoromethyl, etc.) and/or phenyl groups. FL and SV SARD analyses were routine screening of **II** and **III**, along with the binding and antagonism assays described above. SARD activities were determined via Western blots employing NTD directed antibody to determine AR levels. The FL AR and SV AR experiments were performed in LNCaP and 22RV1 cells, respectively, treated at 1 μM and 10 μM, respectively. We have found that, in general, FL AR is more sensitive than SV AR to degradation by **II** and **III**, however, the ability to degrade both is preferable for treating CRPC.

We used Western blot to determine degradation of proteins. As it is difficult to obtain IC₅₀ values due to low throughput nature of the system, we quantified the AR bands and normalized to loading controls and provided as percent degradation. The percent degradation values were segregated into five qualitative ranges of values: 1. no degradation is symbolized as (-) and termed as inactive; 2. < 30% degradation (weak SARD activity) is symbolized as (+); 3. 31% to 60% degradation (moderate SARD activity) is symbolized as (++); 4. 61% to 90% degradation (strong SARD activity) is symbolized as (+++); or 5. > 90% degradation (complete AR degradation) symbolized as (++++). [The terms inactive, weak, moderate, strong and

complete AR degradation and the symbols are used interchangeably.] The SARD SAR discussion below describes the SARD data in Tables 3 and 4. Based on the current data set, it is clear that SARD values for FL (LNCaP) and SV (22RV1) AR are not univocal, which may result in differential efficacy across different PC models. Since the goal is to degrade both FL and SV, these data are discussed in aggregate as SARD activity (see below).

3'-CF₃ (18 series) vs. 3'-Cl (19 series) A-ring: In general, it is unclear whether series **18** (3'-CF₃) or series **19** (3'-Cl) is superior. E.g., comparison in Table 3 of **7** vs. **19c** (both 5-F indoles) and comparison of **18b** vs. **19b** (both 4-F indoles) seem to slightly favor 3'-CF₃. However, it is less clear in the case of 6-F substitution, **18c** (-/+++ for FL/SV) vs. **19d** (+++/- for FL/SV). In general, the substitution with 3'-CF₃ vs. 3'-Cl produced approximately equivocal SARD results.

Indole (18 series and 19 series) vs. Indoline (20 series and 21 series): In many cases only a small advantage is seen for indolines, e.g., **20a** vs. **18a** (both unsubstituted), **20e** vs. **18c** (both 6-F), and **21d** vs. **19d** (both 6-F). However, comparing indoline **21f** vs. indole **19f** (both 5-F, 6-Ph substituted) suggests that the double bond reduction contributes to **21f** SARD activity. Further, both compounds that induced complete (++++) FL degradation were indolines, **21d** and **21f**.

Electron withdrawing groups (EWG) at positions 3-7 of B-ring: In general, electron withdrawal on the B-ring seems to favor the SARD activities of **II** and **III**. For indoles (**II**), compare **19a** (3-F; +++/+++), **7** (5-F; +++/+++), **7r** (*R*-isomer of **7**; 5-F; +++/+++), or **18b-18f** (monofluorination or mononitration at positions 4-6) to the unsubstituted **18a** (+/+++). For indolines (**III**), compare **20b** (4-F; +++/++) and **20e** (6-F; +++/++) to the unsubstituted **20a** (++++/+++). As outlined above, fluorination generally augmented for indoles or retained for

indolines SARD activity relative to the unsubstituted analog. Indoles seemed to benefit more from EWG substitution and fluorination at the 3- (**19a**) or 5- (**7**, **7r**) position is generally optimal. Nitration of the indole ring, e.g., **18e** (5-NO₂) and **18f** (6-NO₂), showed strong SV SARD activity, and very potent *in vitro* antagonism with IC₅₀ values of 0.103 μM and 0.058 μM, respectively, but weaker FL SARD activity. Fluorination at the 4 (**18b**, **19b**, **20b**, **21a**), 5 (**19c**, **21b**), or 6 (**18c**, **19d**, **20e**, **21d**) positions of **II** or **III** produced SARD portfolios with lower % degradation values for FL or SV than **7** (5-F). Larger 5-halogenations on the indole ring (**II**) abolished activity (**18j** (5-Br), **18k** (5-I)), whereas on the indoline ring (**III**) it was better tolerated, e.g., see **21c** (5-Br; ++/-) even though ~1 μM antagonism was seen for all. 5,6-Dihalogenation of 3'CF₃ indolines (**III**) such as **20f** (5,6-diF; +++/++) and **20g** (5-Cl, 6-F; -/-; agonism) did not improve upon the SARD activity over the monohalo analog **20e** (6-F; +++/+++), and further did not conform to the desired screening profile due to partial agonism *in vitro* which represents a liability in the treatment of PC. Contrary to this, **21e** (5,6-diF in the context of 3'-Cl; +++/++) had an improved SARD profile vs. **21b** (5-F; ++/+) and **21d** (6-F; ++++/+) and was a very potent and pure antagonist (0.032 μM). Although **21d** (6-F indoline) produced complete FL AR degradation (and very potent antagonism (0.037 μM)), the SV AR degradation was weak making it a less than ideal compound for CRPC. [Moreover, insertion of a nitrogen atom into the B-ring of **II** (**18n**; 5-CN) produced only weak degradation (+/+) compared to **7** (5-F).]

B-ring 3-position: As suggested above, 3-F (on B-ring) seemed to contribute to SARD activity based on **19a** vs. **18a**, however, the 3'-position (A-ring) is also a variable in this comparison. Also, 3-methylation was tolerated (**18g** vs. **7**), but did not increase activity. Larger substituents, polar and nonpolar, abolished SARD activity completely such as **18l** (3-CO₂H), **18m** (3-CO₂Et), and **19g** (3-Ph, 5-F), possibly suggesting limited steric tolerance. However,

18m and **19g** did retained moderate antagonism of 0.972 μM and 1.032 μM , respectively. This position was not substituted for indolines **III**, but would explore novel structural space due to the tetrahedral carbon.

Addition of phenyl to B-ring: The phenylation of indoles (**II**) was not tolerated at 3, 4, and 5 positions. E.g., see **19g** (3-Ph, 5-F), **18o** (4-Ph), and **18p** (4-F, 5-Ph) in which activity was abolished. This is consistent with steric intolerance at the 3 and 5 positions as discussed above. Steric tolerance at the 6-position of the indole ring is suggested by **18i** (5-F, 6-Ph; ++/+) and **19f** (5-F, 6-Ph; +++/++) where mostly moderate SARD activity was maintained upon addition of 6-Ph group, but lower than **7** (5-F; +++/+++). In contrast, **18q** (4-F, 6-(4-fluorophenyl)) was inactive despite weak antagonism (0.898 μM) and strong binding (0.062 μM). Interestingly, 6-phenylation on the indoline ring (**III**) improved SARD activity, i.e., **21f** (5-F, 6-Ph indoline; ++++/+++) was much improved over **21b** (5-F indoline; ++/+) [or **19c** (5-F indole; +++/+)]. Unlike other indolines, **21f** produced complete FL AR and strong SV AR degradation efficacy, and demonstrated potent antagonism (0.244 μM). The structure of **21f** is reminiscent of the biphenyl B-ring of **3** of class **I**, and may suggest further exploration of the indoline 6-position. **7** (5-F; +++/+++/ 0.085 μM) and **19a** (3-F +++/+++/ 0.045 μM) also produced impressive CRPC *in vitro* screening portfolios.

In vitro metabolic stability in mouse liver microsomes (MLM). Several compounds of each class were selected to be further evaluated for *in vitro* metabolic stability in MLM with co-factors for enzymes of both phase I and phase II metabolism. This allows the calculation of half-life ($T_{1/2}$) and intrinsic clearance (CL_{int}) values as a predictor of the DMPK of series **II** and **III** as shown in Table 5.

In overview, the CL_{int} of **II** and **III** is rapid ($T_{1/2}$ ranges from 9.13 min to 36.32 min), especially compared to **5** (10.04 h in humans; as previously reported)⁵¹ and **2** (360 min in MLM)⁴³ which are orally active and dosed daily in humans. The unsubstituted indole **18a** has a $T_{1/2}$ of 13.66 min. 5-Fluorinated **7** has an equivocal half-life but improved SARD activity (Table 3) whereas 4-fluorination (**18b**; 36.32 min) increased the half-life of **18a** by approximately 3-fold, but reduced SARD activity. In general, 4-substituted indoles, and to a lesser extent, 3- or 5-substituted indoles have improved stability compared to unsubstituted **18a**. This may be due to the steric blocking, or stabilization, of metabolically labile aryl protons on the indole. The most stable SARD reported is **18b** (4-F indole; 36.32 min) is ~3-fold more stable than **18a** (unsubstituted) or **7** (5-F), but this is still far from optimal metabolic stability. Although SARD activity is preserved in some of these longer $T_{1/2}$ compounds, the relative instability of **II** and **III** compared to the standard agents suggested that the pharmacokinetics of these SARDs may need to be vastly improved in order to reveal the *in vivo* pharmacodynamic profile of SARDs **II** and **III**. Nonetheless, **II** and **III** were tested in *in vitro* (e.g., antagonism, SARD, and anti-proliferative assays) and *in vivo* (e.g., xenografts) models of CPRC (e.g., F876L, MR49F, and 22RV1) and demonstrated significant efficacies as will be discussed *infra*. Efforts to improve the SARD efficacy and DMPK characteristics of **II** and **III** are ongoing.

Models of refractory and CRPC

Overview of refractory PC models employed: LNCaP is a well characterized PC cell line which expresses a mutant full-length AR (T877A). The T877A mutation confers resistance to hydroxyflutamide,⁵² but in the absence of other mutants, is sensitive to **5**. 22RV1 cells express both FL AR (H874Y)⁵³ and SV AR (AR-V7). 22RV1 cells demonstrate a more promiscuous ligand binding than wild-type AR (LBD AR) and respond to low levels of androgens and a wide

spectrum of other natural and synthetic steroid hormones, mechanisms proposed to contribute to tumor progression following androgen ablation⁵³. Further, the AR-V7 in 22RV1 supports constitutive AR activity and lacks a LBD such that ADT, abiraterone, and traditional antiandrogens including **5** and **6** cannot block growth of these cells. Our SARD screening employs the combination of LNCaP and 22RV1 cells, respectively, to predict whether a particular SARD can degrade [wildtype] and various escape mutant FL (e.g., T877A, H874Y, W741L, etc.) and SV (e.g., AR-V7 and D567es, etc.) ARs, respectively, which emerge due to treatment with clinically approved antiandrogens. As new agents are approved, new mutant FL and SV AR will be discovered as resistance conferring escape mutants.

Recently, a basis for **5** and **6** resistance was discovered to be either the F876L point mutation or F876F/T877A double mutant. Enz-R MR49F LNCaP cells harbor the double mutant and serve as a model of Enz-R CRPC, which can be tested, e.g., in *in vitro* assays of antagonism of transcriptional activation, SARD activity, or cell anti-proliferation, or as *in vivo* xenografts. Xenografts are particularly informative as they reveal the adequacy of the combination of the pharmacodynamic and DMPK profiles [in the animal species tested] for any given molecule and provide a proof of concept for whether a particular class of agents is ready to be translated toward human testing (e.g., IND-enabling studies such rat and dog toxicity, etc.). We produced CRPC xenografts by growing implanted MR49F cells to 100-300 mm³ in intact animals (i.e., endogenous androgens are present), removing androgens via castration, and re-growing in the absence of androgen. These castration and Enz-R PC xenografts better reflect the CRPC phenotype seen clinically where patients typically are treated with ADT and **5** or **6** and despite this, reactivation of the AR axis occurs. Various members of **II** and **III** demonstrated activity in each of the models described above (see *infra*), including *in vivo* models, despite poor metabolic

stability (Table 5) in the same species, suggesting that metabolically stable SARDs with comparable or improved pharmacodynamic profiles would be promising candidates for treatment of many refractory PC's, including Enz-R CPRC.

***In vitro* models of CRPC: Antagonism, SARD, and antiproliferation in Enz-R cell lines**

SARDs inhibit transcriptional activation of F876L. To validate that **II** and **III** can antagonize the R1881-driven transcriptional activation of mutant AR F876L, we transfected COS cells with F876L AR with a glucocorticoid response element (GRE)-driven luciferase reporter construct, and a Renilla reporter construct as a control for transfection efficiency. The GRE-LUC construct consists of synthetic consensus response elements that are detected by AR, PR, GR, and mineralocorticoid receptor. This construct is widely used in the nuclear receptor field to determine the activity of these receptors. Cells were treated 24 h after transfection with 0.1 nM R1881 (AR agonist) and a dose response of SARDs **II** and **III**. Luciferase (and Renilla) assays were performed 48 h after transfection and reported as relative light units (RLU). COS is not a prostate cancer cell line, so transfection with F876L does not convert them to Enz-R PC. Figure 4A (top middle panel) demonstrated potent (low nM) but not full efficacy antagonism by **5** of R1881-driven F876L transactivation, whereas wt AR inhibition was less potent (low μ M) and full efficacy. Importantly, at high concentrations ($>1 \mu$ M), **5** acts as an agonist of F876L transactivation (top right panel of Figure 4A), which is not seen in wt AR. This is indicative that F876L acts like an agonist switch escape mutant of **5** therapy.

Given that **II** and **III** were structurally novel high potency AR antagonists with a unique biological activity profile, representative compounds [i.e., **7** (5-F indole), **18b** (4-F indole), **18c** (6-F indole), **19c** (5-F indole), **19b** (4-F indole), and **20b** (4-F indoline)] were tested for their

ability to overcome the agonist switch behavior. Approximately equipotent nM range, full efficacy antagonism of R1881-driven transcriptional activation was observed in both F876L and wt. This suggested that our SARDs would also exhibit activity in models of Enz-R (e.g., MR49F cells) and primary PC possessing wt AR.

SARD activity and cellular anti-proliferation in a model of Enz-R PC (MR49F): To ensure that SARD activity was also maintained in a Enz-R cell line, SARD assays were performed in MR49F LNCaP cells containing the F876L/T877A double mutant. As seen in Figure 4B, **19f** (5-F, 6-Ph indole) and **19b** (4-F indole) degraded this mutant FL AR in MR49F cells in the low μM and high nM range, respectively, consistent with the relative activities seen in Tables 3 and 4. Immunoblots suggest that **19b** and/or **19f** demonstrated comparable potency of SARD activity in the Enz-R LNCaP (Figure 4B) when compared to the parental **5** sensitive LNCaP shown *supra* (Figure 3A). This conservation of SARD activity of these compounds suggests that their SARD activity is not highly sensitive to small changes in AR amino acid sequence or the transformed cellular context of the Enz-R cells. **5** was inactive in SARD activity assays in LNCaP (FL) and 22RV1 (SV) cells and was not expected to be a SARD in the MR49F context (or any cellular context), as demonstrated in the lower panel of Figure 4B. The preservation of SARD activity even in the Enz-R context suggested that **II** and **III** may exhibit anti-proliferative and/or anti-tumor activities.

Anti-proliferative assays in MR49F cells showed that **21a** (4-F indoline), **19b** (4-F indole), and **19f** (5-F, 6-Ph indole) completely and dose-dependently inhibited cell growth with estimated IC_{50} values of less than 3 μM for **21a** and **19b**, and less than 1 μM for **19f** (Figure 5A). For **19b** at least, this correlates well with *in vitro* antagonism and SARD activity in MR49F cells (Figure 4), suggesting that **II** and **III** retained their unique biological profile in Enz-R PC. By

comparison, **5** demonstrated weak and incomplete efficacy as revealed by poor dose-dependence and only partial inhibition of growth. E.g., growth inhibitions at 3 μM , 10 μM and 30 μM were approximately 30%, 15%, and 45%. This result demonstrated the Enz-R nature of these MR49F cells, and further affirmed our ability to overcome the Enz-R phenotype with representative examples of **II** and **III**, supporting testing in MR49F xenografts. Further, the AR-dependence of the anti-proliferative action of our SARDs is demonstrated in Figure 5B by the lack of activity of **19b** and **19f** in the AR-negative PC cell line PC-3 at doses as high as 10 μM , removing the possibility of non-specific cytotoxicity underlying anti-proliferative and AR degradation activities.

Reversal of SARD activity in MR49F cells by inhibition of the proteasome: To provide a mechanistic basis for the AR degradation observed with **II** and **III**, we tested the effect of a proteasome inhibitor on AR degradation by **19f** and **19b** in the same model of Enz-R PC as the xenografts (Figure 6). This experiment builds upon the observed AR destabilization by **19f** as shown in Figure S4, discussed *supra*. MR49F cells were treated with **19f** and **19b** in the presence and absence of bortezomib. Cycloheximide, an inhibitor of protein synthesis, was included in all treatments to prevent *de novo* AR synthesis. AR/GAPDH ratios based on densitometric quantitation demonstrate that bortezomib treatment alone (lane 3; ratio of 1.6) increased AR levels compared to vehicle treatment (lane 1; ratio of 1). In contrast, **19f** and **19b** produced comparable high efficacy AR degradation (lanes 2 and 5; ratios of 0.3 and 0.3) that was completely reversed by equimolar bortezomib (lanes 4 and 6; ratios of 1.2 and 0.9) producing AR levels comparable to vehicle treatment. This reversal of **19b**- and **19f**-dependent degradation by bortezomib supports the hypothesis that ubiquitination-dependent proteasomal degradation is enhanced by **19b** and **19f**. The ubiquitin-proteasome system is a tightly

regulated, highly specific pathway responsible for the vast majority of protein turnover within the cell. The ability to target the AR to the ubiquitin-proteasomal pathway even in this model of EnzR PC helps to rationalize the anti-tumor activity (discussed *infra*) observed despite poor PK properties.

***In vivo* antagonism: Hershberger assays and enzalutamide resistant LNCaP xenografts**

Hershberger assays. Uncertain of whether our combination of pharmacodynamic (pan-antagonism and pan-SARD activities) and pharmacokinetic (e.g., poor stability in MLM) properties would be sufficiently robust to observe AR antagonism *in vivo*, we performed Hershberger assays on several selected **II** and **III** orally administered in intact mice and rats. Surprisingly, despite poor MLM stabilities, the tested SARDs (**21a**, **21b**, **18c**, **19f**, **7**, **19b**, **19c**, **19a** and **21f**) caused atrophy of AR-dependent seminal vesicles tissue in intact mice (Figure 7A, left panels) whereas vehicle did not have any effect (0% change). Similar efficacy atrophy was also observed for **21a** and **21b** in rats (Figure 7A, right panel) and was demonstrated to be dose-dependent in prostate and seminal vesicles, with up to ~40% change in organ weights relative to castrated control (100%). Though only partial efficacy at 40 mg per kg, this confirms that orally administered compounds are being absorbed and distributed to the site of action in these organs and suggests that these compounds should also distribute to tumors in xenograft models to exert anti-tumor effects in sensitive models.

MR49F Xenografts in mice: Following the demonstration of *in vitro* activity in MR49F and *in vivo* antagonism in Hershberger assays, there was confidence in our ability to demonstrate activity in Enz-R xenografts. MR49F xenograft experiments were completed with **19f** and **19b**. **19b** and **19f** satisfied all the criteria for a next generation AR antagonist for EnzR PC that

includes stronger AR-LBD binding, lower AR antagonistic IC₅₀, better degradation of AR and AR-SV degradation than enzalutamide. **19b** was the best 3'-Cl indole (**19** series) *in vitro* (Table 3), however **19f** produced superior *in vivo* antagonism in intact animals (Figure 7A), despite non-optimal *in vitro* values. Hence, we chose **19b** and **19f** for further characterization to see whether *in vitro* or *in vivo* data was more predictive of anti-cancer activity.

MR49F xenografts were established by implanting these Enz-R LNCaP cells (a kind gift from Dr. Martin Gleeve, University of British Columbia) mixed with Matrigel (BD Biosciences, San Jose, CA) at 1:1 ratio and injecting subcutaneously in NOD SCID gamma (NSG) mice. Once tumor sizes reached 100-200 mm³, the mice were castrated and the tumors were allowed to regrow as CRPC. The animals were randomized once the tumors started to regrow and treated with vehicle (polyethylene glycol-300:DMSO 85:15 ratio) or 100 mg per kg of SARDs **19f** or **19b** for 14 d. In Figure 7B, **19f** and **19b** significantly reduced the tumor volume with a 40-60% tumor growth inhibition (TGI), whereas **5** did not significantly reduce the growth of MR49F xenografts. Though almost equivocal, **19f** appeared to perform slightly better than **19b** in this proof-of-concept experiment, possibly suggesting *in vivo* data was a better predictor of anti-cancer activity.

Further, the significant levels of TGI activity indicated that the oral bioavailability demonstrated in Hershberger assays translated to adequate levels of **19f** and **19b** in tumor to reveal [at least to some extent] the pharmacodynamic behavior of our SARDs. Though complete tumor regression was not accomplished as may be possible with improved pharmacokinetic properties, the proof-of-concept that our SARDs can overcome Enz-R CRPC *in vivo* was established through the susceptibility of these Enz-R xenografts to **19f** and **19b**. This promising result is surprising given the poor metabolic stability of **II** and **III** as a whole in the same species

(mice) as seen in MLM (Table 5; $T_{1/2}$ for **19f** and **19b** were 9.13 min and 11.77 min). These experiments provide hope that our SARDs with their unique biological profile could be used to overcome **5** and by extension **6** and abiraterone resistances in CRPC patients.

3. CONCLUSIONS AND DISCUSSION

In our effort to find bioactive small molecules for the treatment of advanced prostate cancers (PCs), a novel series of indolyl and indolinyl propanamides (series **II** and **III**, respectively) were discovered to be selective androgen receptor degraders (SARDs). The first generation of SARDs were metabolically labile secondary and tertiary amines (**I**) lacking *in vivo* activity that were designed by structural modification of the androgen receptor (AR) antagonist **1** [2-hydroxy-4-(4-isothiocyanatophenyl)-2-methyl-*N*-(4-nitro-3-(trifluoromethyl)phenyl)butanamide] and tissue-selective AR agonist enobosarm (**2**, (*S*)-*N*-(4-cyano-3-(trifluoromethyl)phenyl)-3-(4-cyanophenoxy)-2-hydroxy-2-methylpropanamide). Class **I** was exemplified by **3** [(*S*)-*N*-(4-cyano-3-(trifluoromethyl)phenyl)-3-((6-cyano-[1,1'-biphenyl]-3-yl)(methyl)amino)-2-hydroxy-2-methylpropanamide] whose tertiary amine was cyclized to form indoles (**II**) and indolines (**III**). **II** and **III** are characterized herein as potent AR antagonists and SARDs with a broad activity profile in models of PC, and *in vivo* AR antagonism when orally administered. E.g., SARDs of **II** and **III** exhibited strong AR antagonistic activity *in vitro* in transcriptional activation and cellular proliferative assays including in models of **5** sensitive and resistant PCs, and castration resistant PCs (CRPCs).

Additionally, **II** and **III** showed selective AR [protein] degradation of FL (e.g., from LNCaP cells (T877A)) and SV (e.g., from 22RV1 cells (AR-V7)) isoforms of AR, all at sub to

low micromolar treatment levels, and in a variety of prostate cancer cell contexts including Enz-R PCs (e.g., MR49F). The ability to degrade SV AR in this study suggested the potential of **II** and **III** to treat various currently untreatable advanced and refractory PCs. E.g., those lacking the LBD of AR such as AR-V7 and D567es AR truncations, which are not susceptible to ADT, abiraterone, or LBD-directed antiandrogens (e.g., **4-6**), and are associated with short survival.²¹

⁵⁴ Further, *in vivo* investigations found that analogs within the **II** and **III** series overcome a variety of escape mutants including F876L and F876L/T877A (MR49F) that are known to emerge due to enzalutamide (**5**) treatment. These mutations convert **5** and **6** to agonists, conferring resistance to PC cells and tumors²² via an agonist switch mechanism as seen with other LBD-binding antiandrogens, e.g. W741L for **4** and T877A for flutamide (*N*-(4-nitro-3-(trifluoromethyl)phenyl)isobutyramide). The intractability of truncation mutants and the frequency of the agonist switch mutations suggest that novel ways, potentially LBD-independent ways, of targeting the AR are needed. The design, synthesis and biological evaluation of these SARDs as putative treatments of Enz-R and other advanced PCs is discussed. Moreover, these orally bioavailable SARDs are dual acting agents, i.e., potent inhibitors and degraders of AR, providing a higher evolutionary barrier to the development of resistance to **II** and **III**. For all these reasons, we believe that *N*-terminally directed SARDs²⁸ may provide a next generation of AR antagonists to treat a variety of refractory and/or advanced prostate cancers, including Enz-R, castration resistant, and/or AR-V7 dependent PCs which are not amendable with current hormone therapies. As such, SARDs may delay the need to rely solely on chemotherapy.

The lack of satisfactory hormonal pharmacotherapy for metastatic patients that have failed to respond to abiraterone and/or **5** and **6** [approved in February 2018] has piqued interest in the development of therapies to overcome Enz-R AR mutations. Some of the promising

preclinical approaches include: 1.) combination therapies, e.g., sorafenib⁵⁵ or CDK-4/6 inhibitors⁵⁶ with **5** to revert the Enz-R phenotype; or 2.) AR-directed monotherapies such as the emerging PROTACs technology that exploits cellular quality control machinery to selectively degrade specific target proteins⁵⁷⁻⁵⁸ by creating in this case AR-PROTAC-E3 ubiquitin ligase ternary complexes; or 3.) AR-independent approaches to treat CRPC, e.g., by activating Natural Killer (NK) cells to attack the cancer⁵⁹; and each have shown promise in Enz-R or AR-V7 CRPC preclinical models. These approaches are still early in their development cycles, and many technical and regulatory hurdles remain for these approaches before any might reach the clinic for Enz-R patients. Other drugs in the clinical pipeline such as second generation antiandrogens, e.g., darolutamide (OEM-201)⁶⁰, are just LBD-directed antiandrogens like **5** that will be susceptible to single amino acid and truncation escape mutations as observed for **5** and **6** and all first generation antiandrogens. Further, in the final analysis, none of the above may be approved which would leave no viable alternatives to taxanes in antiandrogen resistant CRPC.

Importantly, to date none of the approaches mentioned above are dual targeted antagonists capable of inhibiting and destroying various FL and SV ARs including all escape mutants tested to date. Herein we report for the first time, an initial SAR series for our SARD program for the indole (**II**) and indoline (**III**) SARDs described above that are capable of destroying FL and SV ARs with high efficacy. Herein and recently,²⁸ we characterized several members of groups **I-III** as having a unique biological activity profile optimized to address Enz-R CRPC. E.g., these compounds:

- 1) Generally bind to LBD of wt AR;
- 2) Inhibit transcriptional activation of wt AR (Tables 1, 3, and 4), escape mutant ARs (F876L in Figure 4A, and T877A, Q711A, L704A, and N705A), and SV AR;²⁸

- 3) Exert high efficacy and potency SARD activity against FL and SV AR whether wildtype or harboring point-mutations (LNCaP in Tables 1, 3, and 4) or truncations (22RV1 in Tables 1, 3, and 4; LNCaP-95 and D567es cells²⁸), including an Enz-R cellular context (e.g., MR49F in Figure 4B);
- 4) Exert AR antagonism *in vivo* when administered orally in intact animals (Figure 7A);
- 5) Exert PC anti-proliferative activity *in vitro* (Figure 5) and *in vivo* (see LNCaP, 22RV1, and Pr-3001 xenografts²⁸) including in Enz-R CRPC (Figure 7B); and
- 6) Bind to a secondary binding site in AF-1 believed to mediate SARD activity as demonstrated in Supplemental Figure S2 for **19b** by fluorescence polarization and for **3** and **7** by fluorescence polarization and NMR studies.²⁸

This broad spectrum of androgen antagonism is itself unprecedented. It is not possible at present to definitively assert that SARD activity alone is responsible for the activity seen in Enz-R cells and tumors. E.g., SARD activity *in vitro* does not necessarily correlate with *in vivo* AR antagonism as seen with **19b** vs. **19f** where **19b** would be the *in vitro* lead candidate and **19f** would be the *in vivo* lead candidate. We tested both and found equivocal Enz-R xenograft efficacy, leaving this an open question. Though **I-III** suffer from a lack of metabolic stability in MLM, it was still possible to observe *in vivo* antagonism in mice in the seminal vesicles weight (an androgenic target organ) and in Enz-R xenografts. Given the poor DMPK properties of **II** and **III**, we believe that additional SAR exploration to further co-optimize the SARD/antagonism and DMPK properties will reveal an even more promising *in vivo* pharmacodynamic profile. Further, it is our belief that this pharmacodynamic profile will be more resilient to the development of resistance, because:

- 1) SARD activity is effective against a variety of FL point mutations and SV AR truncations which lack the LBD, hence the development of resistance by these mechanisms may be thwarted or greatly delayed;
- 2) SARD activity is mediated through a binding site in the NTD, further indicating that SV and LBD point mutations will not prevent SARD activity;
- 3) SARD activity should be able to overcome resistance due to AR gene amplifications or intratumoral androgen synthesis by eliminating the binding site for endogeneous androgens;
- 4) These agents are also potent antagonists of FL and SV transcriptional activations, allowing inhibition of any residual AR left due to incomplete AR degradation and/or the emergence of novel types of resistance to the SARD activity.

Although Enz-R is the initial target population, these agents may also be promising in early stage PC because of the multiple barriers to the development of resistance. The optimization of this template and the exploration of other templates of NTD-directed SARDs is ongoing, with improved bioavailabilities seen in other templates (to be published separately). Cumulatively, it is our belief that NTD-directed SARDs, because of their unique mechanism and broad scope biological activity profile may be able to resurrect the AR-axis as a viable target, even after current antiandrogens have been tried and failed.

4. EXPERIMENTAL SECTION

General Chemistry Methods. All chemicals for synthesis were purchased from Sigma-Aldrich Chemical Co., Fisher Scientific (Pittsburgh, PA), Matrix Scientific (Columbia, SC), AK Scientific (Mountain View, CA), Oakwood Products (West Columbia, SC) etc. and used without

further purification. Moisture-sensitive reactions were carried under an argon atmosphere. Analytical thin-layer chromatography (TLC) was carried out on pre-coated silica gel (Merck Kieselgel 60 F₂₅₄ layer thickness 0.25 mm). NMR spectra were obtained on a Bruker Avance III 400 (Billerica, MA) spectrometer. Chemical shifts are reported as parts per million (ppm) relative to TMS in CDCl₃ or DMSO-*d*₆. The structure of synthesized compounds was also assigned by ¹H-¹H 2D-COSY and 2D-NOE NMR analytic methods. Flash column chromatography was performed on using silicagel (230-400 mesh, Merck). Mass spectral data was collected on a Bruker Esquire-LC/MS system (Bruker Daltonics, Billerica, MA) equipped with electrospray/ion trap instrument in positive and negative ion modes (ESI source). The purity of the final compounds was analyzed by an Agilent 1100 HPLC system (Santa Clara, CA). HPLC conditions: 45% acetonitrile at flow rate of 1.0 mL/min using a LUNA 5 μ C18 100A column (250 × 4.60 mm) purchased from Phenomenex (Torrance, CA) at ambient temperature. UV detection was set at 340 nm or 245 nm. Purities of the compounds were established by careful integration of areas for all peaks detected and determined as ≥95% for all compounds tested for biological study.

General Procedure: Method A (for Class II indole derivatives, 18a ~ 18q, 19a ~ 19g).

Under argon atmosphere, NaH of 60% dispersion in mineral oil (228 mg, 5.7 mmol) was added in 30 mL of anhydrous THF solution of substituted indole **16** (2.84 mmol) in 100 mL dried two necked round bottom flask equipped with a dropping funnel at ice-water bath, and the resulting solution was stirred 30 min at the ice-water bath (Scheme 1). Into the flask, the prepared solution of epoxide **14** or **15** (2.84 mmol in THF) was added through dropping funnel under argon atmosphere at the ice-water bath and stirred overnight at room temperature. After adding 1 mL of H₂O, the reaction mixture was condensed under reduced pressure, and then dispersed into 50 mL

of EtOAc, washed with 50 mL (x 2) water, evaporated, dried over anhydrous MgSO₄, and evaporated to dryness. The mixture was purified with flash column chromatography as an eluent EtOAc / hexane to produce the desired indole series **II**.

General Procedure: Method B (for Class III indoline derivatives, 20a ~ 20g, 21a ~ 21f). Under argon atmosphere, 2.0 M lithium diisopropylamide solution (4.6 mL, 4.6 mmol) in THF/heptane/ethylbenzene was slowly added in a dropwise manner over 10 min to a solution of substituted indoline **17** (2.2 mmol) in 5 mL of anhydrous THF at -78 °C and warmed to 0 °C and stirred for 10 min and cooled again to -78 °C (Scheme 1). To the solution was added in a dropwise fashion to a solution of epoxide **14** or **15** (2.2 mmol) prepared from compounds **12** or **13**, and the reaction mixture was stirred for overnight. After quenching by addition of sat. NH₄Cl, the solution was concentrated under reduced pressure and dispersed into excess EtOAc and dried over Na₂SO₄. The solution was concentrated and purified by flash column chromatography (EtOAc/hexane or DCM/hexane) to give the desired indoline series compound of **III**.

Synthesis and Analysis of Compounds. Preparation of a solution of (*S*)-*N*-aryl-2-methyloxirane-2-carboxamide (**14** or **15**): A mixture of hydroxybromide **12** or **13** (2.84 mmol) and potassium carbonate (5.70 mmol) in 60 mL acetone was heated to reflux for 30 min. After complete conversion of starting bromide **12** or **13** to desired intermediate epoxide **14** or **15** as monitored by TLC, the solvent was evaporated under reduced pressure to give yellowish residue, which was poured into 20 mL of anhydrous EtOAc (Scheme 1). The solution was filtered through Celite pad to remove K₂CO₃ residue and condensed under reduced pressure to give a yellowish solid of epoxide, which was dissolved in 5 mL of anhydrous THF to prepare a desired solution of epoxide in THF. The resulting solution was directly used as next reactant without analysis

(S)-N-(4-Cyano-3-(trifluoromethyl)phenyl)-2-methyloxirane-2-carboxamide (14).

Light yellowish solid. Yield = 95%; MS (ESI) m/z 269.5 [M – H]⁻; ¹H NMR (CDCl₃, 400 MHz) δ 8.68 (bs, 1H, NH), 8.10 (s, 1H), 7.95 (d, J = 8.4 Hz, 1H), 7.79 (d, J = 8.4 Hz, 1H), 3.02 (d, J = 4.8 Hz, 1H), 2.98 (d, J = 4.8 Hz, 1H), 1.65 (s, 3H); ¹⁹F NMR (CDCl₃, decoupled) δ -62.23.

(S)-N-(3-Chloro-4-cyanophenyl)-2-methyloxirane-2-carboxamide (15). Yield = 92% ; MS (ESI) m/z 316.86 [M – H]⁻; ¹H NMR (CDCl₃, 400 MHz) δ 8.86 (bs, 1H), 7.97 (d, J = 2.0 Hz, 1H), 7.64 (d, J = 8.8 Hz, 1H), 7.54 (dd, J = 8.8, 2.0 Hz, 1H), 4.02 (d, J = 10.8 Hz, 1H), 3.60 (d, J = 10.8 Hz, 1H), 2.99 (s, OH, 1H), 1.58 (s, 3H); ¹³C NMR (CDCl₃, 100 MHz) δ 171.3, 141.8, 138.0, 120.3, 117.7, 115.9, 108.6, 75.5, 41.2, 24.8.

5-Fluoro-6-phenyl-1H-indole (16a). To a suspension of tetrakis(triphenylphosphine)palladium(0) [Pd(PPh₃)₄, 0.54 g, 0.467 mmol] in 20 mL of ethylene glycol dimethyl ether (DME) was added 6-bromo-5-fluoroindole (1.00 g, 4.67 mmol), and the mixture was stirred for 15 minutes under argon at room temperature. A solution of phenylboronic acid (0.57 g, 4.67 mmol) in 2-3 mL of ethanol was added and the mixture was stirred for 10 minutes under the same conditions. A solution of potassium carbonate (0.97 g, 7.01 mmol) in 2 mL of water was added to the above mixture and the resulting reaction mixture was heated at reflux for 3-4 h under the argon atmosphere. The end of the reaction was established by TLC. The reaction was diluted by brine, and extracted with ethyl acetate. The organic layer was washed with brine, dried with MgSO₄, filtered, and concentrated under vacuum. The product was purified by a silica gel column using ethyl acetate and hexanes (1:3, v/v) as an eluent to afford 0.90 g (yield 92%) of the titled compound as light brown solid.

4-Phenyl-1H-indole (16b). To a suspension of tetrakis(triphenylphosphine)palladium(0) [Pd(PPh₃)₄, 1.179 g, 1.0212 mmol] in 40 mL of ethylene glycol dimethyl ether (DME) was

added 4-bromo-indole (2.00 g, 10.202 mmol), and the mixture was stirred for 15 minutes under argon at room temperature. A solution of phenylboronic acid (1.24 g, 10.202 mmol) in 4.5 mL of ethanol was added and the mixture was stirred for 10 minutes under the same conditions. A solution of potassium carbonate (2.16 g, 15.306 mmol) in 3.5 mL of water was added to the above mixture and the resulting reaction mixture was heated at reflux for 3-4 h under the argon atmosphere. After the end of the reaction was established by TLC, the reaction was diluted by brine, and extracted with ethyl acetate. The organic layer was washed with brine, dried with MgSO₄, filtered, and concentrated under vacuum. The product was purified by a silica gel column using ethyl acetate and hexane (1:3 to 2:1, v/v) as eluent to afford 1.67 g (yield 84.8%) of the titled compound as yellowish oil.

4-Fluoro-6-(4-fluorophenyl)-1H-indole (16c). To a suspension of tetrakis(triphenylphosphine)palladium(0) [Pd(PPh₃)₄, 270 mg, 0.2336 mmol] in 10 mL of ethylene glycol dimethyl ether (DME) was added 6-bromo-4-fluoro-indole (0.50 g, 2.336 mmol), and the mixture was stirred for 15 minutes under argon at room temperature. A solution of 4-fluoro-phenylboronic acid (0.33 g, 2.336 mmol) in 1.2 mL of ethanol was added and the mixture was stirred for 10 minutes under the same conditions. A solution of potassium carbonate (0.48 g, 3.504 mmol) in 1.0 mL of water was added to the above mixture and the resulting reaction mixture was heated at reflux for 3-4 h under argon atmosphere. After the end of the reaction was established by TLC, the reaction was diluted by brine, and extracted with ethyl acetate. The organic layer was washed with brine, dried with MgSO₄, filtered, and concentrated under vacuum. The product was purified by a silica gel column using ethyl acetate and hexane (1:3, v/v) as an eluent to afford 0.33 g (yield 61.6%) of the titled compound as brown solid.

(S)-N-(4-Cyano-3-(trifluoromethyl)phenyl)-2-hydroxy-3-(1H-indol-1-yl)-2-methylpropanamide (18a). By Method A: Yield 55%; Light brown solid; MS (ESI) m/z 358.9 [M - H]⁻; ¹H NMR (CDCl₃, 400 MHz) δ 8.67 (bs, 1H, NH), 7.96 (dd, J = 8.4, 2.0 Hz, 1H), 7.80 (s, 1H), 7.71-7.65 (m, 2H), 7.51 (d, J = 8.0 Hz, 1H), 7.35 (d, J = 8.0 Hz, 1H), 7.12 (t, J = 8.0 Hz, 1H), 7.02 (m, 1H), 6.45 (d, J = 3.2 Hz, 1H), 4.58 (d, J = 14.8 Hz, 1H), 4.30 (d, J = 14.8 Hz, 1H), 2.50 (bs, 1H, OH), 1.54 (s, 3H).

(S)-N-(4-Cyano-3-(trifluoromethyl)phenyl)-3-(4-fluoro-1H-indol-1-yl)-2-hydroxy-2-methylpropanamide (18b). By Method A: Yield 49%; White solid; MS (ESI) m/z 404.1 [M - H]⁻; ¹H NMR (CDCl₃, 400 MHz) δ 8.78 (bs, 1H, NH), 7.92 (s, 1H), 7.78 (m, 2H), 7.23 (d, J = 8.0 Hz, 1H), 7.14-7.11 (m, 2H), 6.78 (dd, J = 10.0, 2.0 Hz, 1H), 6.63 (d, J = 2.8 Hz, 1H), 4.67 (d, J = 14.8 Hz, 1H), 4.39 (d, J = 14.8 Hz, 1H), 2.60 (bs, 1H, OH), 1.65 (s, 3H).

(S)-N-(4-Cyano-3-(trifluoromethyl)phenyl)-3-(6-fluoro-1H-indol-1-yl)-2-hydroxy-2-methylpropanamide (18c). By Method A: Yield 48%; White solid; MS (ESI) m/z 404.0 [M - H]⁻; ¹H NMR (CDCl₃, 400 MHz) δ 8.79 (bs, 1H, NH), 7.89 (d, J = 1.6 Hz, 1H), 7.83 (d, J = 8.4 Hz, 1H), 7.77 (d, J = 8.0 Hz, 1H), 7.51 (dd, J = 8.4, 5.2 Hz, 1H), 7.14 (dd, J = 10.0, 2.0 Hz, 1H), 7.11 (d, J = 3.2 Hz, 1H), 6.87 (dt, J = 8.8, 2.0 Hz, 1H), 6.51 (d, J = 3.2 Hz, 1H), 4.62 (d, J = 14.8 Hz, 1H), 4.32 (d, J = 14.8 Hz, 1H), 2.56 (bs, 1H, OH), 1.65 (s, 3H).

(S)-N-(4-Cyano-3-(trifluoromethyl)phenyl)-2-hydroxy-2-methyl-3-(5-nitro-1H-indol-1-yl)propanamide (18e). By Method A: Yield 47%; Yellowish solid; MS (ESI): 431.0 [M - H]⁻; ¹H NMR (Acetone-*d*₆, 400 MHz) δ 9.68 (bs, 1H, NH), 8.35 (d, J = 2.0 Hz, 1H), 8.16 (s, 1H), 8.01 (m, 1H), 7.88-7.81 (m, 2H), 7.58 (d, J = 8.8 Hz, 1H), 7.38 (d, J = 3.4 Hz, 1H), 6.58 (d, J = 3.4 Hz, 1H), 5.49 (s, 1H, OH), 4.66 (d, J = 14.8 Hz, 1H), 4.38 (d, J = 14.8 Hz, 1H), 1.50 (s, 3H).

(S)-N-(4-Cyano-3-(trifluoromethyl)phenyl)-2-hydroxy-2-methyl-3-(6-nitro-1H-indol-1-yl)propanamide (18f). By Method A: Yield 31%; MS (ESI) m/z 431.1 [M – H]⁻; ¹H NMR (400 MHz, CDCl₃) δ 8.87 (bs, 1H, NH), 8.53 (m, 1H), 8.01 (dd, J = 8.8, 2.0 Hz, 1H), 7.92 (d, J = 2.0 Hz, 1H), 7.86 (dd, J = 8.4, 2.0 Hz, 1H), 7.78 (d, J = 8.4 Hz, 1H), 7.64 (d, J = 8.8 Hz, 1H), 7.43 (d, J = 3.0 Hz, 1H), 6.61 (d, J = 3.0 Hz, 1H), 4.76 (d, J = 14.8 Hz, 1H), 4.48 (d, J = 14.8 Hz, 1H), 3.14 (s, 1H, OH), 1.74 (s, 3H).

(S)-N-(4-Cyano-3-(trifluoromethyl)phenyl)-3-(5-fluoro-3-methyl-1H-indol-1-yl)-2-hydroxy-2-methylpropanamide (18g). By Method A: Yield 64%; MS (ESI) m/z 418.1 [M – H]⁻; ¹H NMR (400 MHz, CDCl₃) δ 8.85 (bs, 1H, NH), 7.86 (m, 1H), 7.81-7.74 (m, 2H), 7.29 (dd, J = 9.0, 4.0 Hz, 1H), 7.14 (dd, J = 9.0, 2.4 Hz, 1H), 6.92 (m, 2H), 4.60 (d, J = 15.2 Hz, 1H), 4.27 (d, J = 15.2 Hz, 1H), 2.22 (s, 3H), 1.57 (s, 3H).

(S)-N-(4-Cyano-3-(trifluoromethyl)phenyl)-3-(5-fluoro-6-phenyl-1H-indol-1-yl)-2-hydroxy-2-methylpropanamide (18i). By Method A: To a solution of 5-fluoro-6-phenyl-1H-indole (**16a**, 370 mg, 1.75 mmol) in anhydrous THF (10 mL), which was cooled in an ice water bath under an argon atmosphere, was added sodium hydride (60% dispersion in oil, 0.11 g, 2.63 mmol). After addition, the resulting mixture was stirred for three hours. (S)-N-(4-Cyano-3-(trifluoromethyl)phenyl)-2-methyloxirane-2-carboxamide (**14**, 470 mg, 2.175 mmol) was added to above solution, and the resulting reaction mixture was allowed to stir overnight at room temperature under argon. The reaction was quenched by water, and extracted with ethyl acetate. The organic layer was washed with brine, dried with MgSO₄, filtered, and concentrated under vacuum. The product was purified by a silica gel column using ethyl acetate and hexane (1:2, v/v) as eluent to afford 830 mg (yield 98%) of the titled compound as off-white foam. ¹H NMR (400 MHz, DMSO-*d*₆) δ 10.29 (s, 1H, NH), 8.28 (s, 1H, ArH), 8.08 (d, J = 8.8 Hz, 1H, ArH),

7.96 (d, $J = 8.8$ Hz, 1H, ArH), 7.58 (d, $J = 6.8$ Hz, 1H, ArH), 7.49-7.31 (m, 7H, ArH), 6.42 (d, $J = 3.2$ Hz, 1H, ArH), 6.35 (s, 1H, OH), 4.61 (d, $J = 14.4$ Hz, 1H, CH), 4.35 (d, $J = 14.4$ Hz, 1H, CH), 1.46 (s, 3H, CH₃).

(S)-3-(5-Bromo-1H-indol-1-yl)-N-(4-cyano-3-(trifluoromethyl)phenyl)-2-hydroxy-2-methylpropanamide (18j). By Method A: Yield 71%; MS (ESI) 465.1 [M - H]⁻; ¹H NMR (CDCl₃, 400 MHz) δ 8.73 (bs, 1H, NH), 7.88 (s, 1H), 7.74 (d, $J = 1.8$ Hz, 1H), 7.69 (d, $J = 1.8$ Hz, 1H), 7.30 (d, $J = 8.8$ Hz, 1H), 7.24 (m, 1H), 7.24 (dd, $J = 8.8, 2.0$ Hz, 1H), 7.13 (d, $J = 3.2$ Hz, 1H), 6.45 (d, $J = 3.2$ Hz, 1H), 4.39 (d, $J = 14.8$ Hz, 1H), 2.60 (bs, 1H, OH), 1.65 (s, 3H).

(S)-N-(4-Cyano-3-(trifluoromethyl)phenyl)-2-hydroxy-3-(5-iodo-1H-indol-1-yl)-2-methylpropanamide (18k). By Method A: Yield 74%; MS (ESI) m/z 511.9 [M - H]⁻; ¹H NMR (CDCl₃, 400 MHz) δ 8.71 (bs, 1H, NH), 7.91 (d, $J = 1.6$ Hz, 1H), 7.74 (m, 2H), 7.43 (dd, $J = 8.8, 1.6$ Hz, 1H), 7.21 (d, $J = 8.8$ Hz, 1H), 7.08 (d, $J = 3.2$ Hz, 1H), 6.44 (d, $J = 3.2$ Hz, 1H), 4.62 (d, $J = 15.0$ Hz, 1H), 4.32 (d, $J = 15.0$ Hz, 1H), 2.44 (bs, 1H, OH), 1.61 (s, 3H).

(S)-Ethyl 1-(3-((4-cyano-3-(trifluoromethyl)phenyl)amino)-2-hydroxy-2-methyl-3-oxopropyl)-1H-indole-3-carboxylate (18m). By Method A: Yield 92%; MS (ESI) m/z 458.1 [M - H]⁻; 482.4 [M + Na]⁺; ¹H NMR (400 MHz, CDCl₃) δ 8.86 (bs, 1H, NH), 8.00 (m, 2H), 7.81 (s, 1H), 7.65 (s, 2H), 7.46 (d, $J = 8.0$ Hz, 1H), 7.24-7.18 (m, 2H), 4.65 (d, $J = 14.4$ Hz, 1H), 4.39 (d, $J = 14.4$ Hz, 1H), 4.36 (bs, 1H, OH), 4.23-4.11 (m, 2H), 1.66 (s, 3H), 1.35 (t, $J = 7.2$ Hz, 3H).

(S)-3-(5-Cyano-1H-pyrrolo[3,2-*b*]pyridin-1-yl)-N-(4-cyano-3-(trifluoromethyl)phenyl)-2-hydroxy-2-methylpropanamide (18n). By Method A: Yield 67%; White solid; MS (ESI) m/z 412.1 [M - H]⁻; 436.1 [M + Na]⁺; ¹H NMR (400 MHz, Acetone-*d*₆) δ 9.84 (bs, 1H, NH), 8.31 (s, 1H), 8.14 (m, 2H), 8.01 (m, 1H), 7.81 (d, $J = 2.8$ Hz, 1H), 7.60 (d,

$J = 8.4$ Hz, 1H), 6.67 (d, $J = 2.8$ Hz, 1H), 5.64 (bs, 1H), 4.84 (d, $J = 14.8$ Hz, 1H), 4.52 (d, $J = 14.8$ Hz, 1H), 1.66 (s, 3H).

(S)-N-(4-Cyano-3-(trifluoromethyl)phenyl)-2-hydroxy-2-methyl-3-(4-phenyl-1H-indol-1-yl)propanamide (18o). By Method A: To a solution of 4-phenyl-1H-indole (**16b**, 0.42 g, 2.173 mmol) in anhydrous THF (10 mL), which was cooled in an ice water bath under an argon atmosphere, was added sodium hydride (60% dispersion in oil, 0.22 g, 5.434 mmol). After addition, the resulting mixture was stirred for three hours. (S)-N-(4-cyano-3-(trifluoromethyl)phenyl)-2-methyloxirane-2-carboxamide (**14**, 0.76 g, 2.173 mmol) was added to the above solution, and the resulting reaction mixture was allowed to stir overnight at room temperature under argon. The reaction was quenched by water, and extracted with ethyl acetate. The organic layer was washed with brine, dried with MgSO₄, filtered, and concentrated under vacuum. The product was purified by a silica gel column using ethyl acetate and hexane (1:2, v/v) as eluent to afford 0.69 g (yield 69%) of the titled compound as off-white solid. ¹H NMR (400 MHz, DMSO-*d*₆) δ 10.37 (s, 1H, NH), 8.37 (d, $J = 2.0$ Hz, 1H, ArH), 8.18 (dd, $J = 8.4$ Hz, $J = 2.0$ Hz, 1H, ArH), 8.05 (d, $J = 8.4$ Hz, 1H, ArH), 7.60-7.54 (m, 3H, ArH), 7.49-7.45 (m, 2H, ArH), 7.38-7.34 (m, 2H, ArH), 7.18-7.14 (m, 1H, ArH), 7.04 (d, $J = 7.2$ Hz, 1H, ArH), 6.51 (d, $J = 3.2$ Hz, 1H, ArH), 6.35 (s, 1H, OH), 4.58 (d, $J = 14.4$ Hz, 1H, CH), 4.38 (d, $J = 14.4$ Hz, 1H, CH), 1.45 (s, 3H, CH₃). MS (ESI, Positive) m/z 464.1536 [M + H]⁺; 486.1351 [M + Na]⁺.

(S)-N-(4-Cyano-3-(trifluoromethyl)phenyl)-3-(4-fluoro-5-phenyl-1H-indol-1-yl)-2-hydroxy-2-methylpropanamide (18p). By Method A: To a solution of 4-fluoro-5-phenyl-1H-indole (330 mg, 0.00156mol) in anhydrous THF (10 mL), which was cooled in an ice water bath under an argon atmosphere, was added sodium hydride (60% dispersion in oil, 160 mg, 3.91 mmol). After addition, the resulting mixture was stirred for three hours. (S)-N-(4-Cyano-3-

(trifluoromethyl)phenyl)-2-methyloxirane-2-carboxamide **14** (550 mg, 1.56 mmol) was added to the above solution, and the resulting reaction mixture was allowed to stir overnight at room temperature under argon. The reaction was quenched by water, and extracted with ethyl acetate. The organic layer was washed with brine, dried with MgSO₄, filtered, and concentrated under vacuum. The product was purified by a silica gel column using ethyl acetate and hexanes (1:2, v/v) as eluent to afford 470 mg (yield 63%) of the titled compound as off-white solid. ¹H NMR (400 MHz, DMSO-*d*₆) δ 10.33 (s, 1H, NH), 8.35 (d, *J* = 2.0 Hz, 1H, ArH), 8.17 (dd, *J* = 8.4, 2.0 Hz, 1H, ArH), 8.05 (d, *J* = 8.4 Hz, 1H, ArH), 7.51-7.40 (m, 5H, ArH), 7.36-7.32 (m, 2H, ArH and indole-H), 7.17-7.13 (m, 1H, ArH), 6.53 (d, *J* = 3.2 Hz, 1H, ArH), 6.38 (s, 1H, OH), 4.60 (d, *J* = 14.8 Hz, 1H, CH), 4.38 (d, *J* = 14.8 Hz, 1H, CH), 1.45 (s, 3H, CH₃); MS (ESI, Negative) *m/z* [M - H]⁻; (ESI, Positive): 482.1490 [M + H]⁺; 504.1310 [M + Na]⁺.

(S)-N-(4-Cyano-3-(trifluoromethyl)phenyl)-3-(4-fluoro-6-(4-fluorophenyl)-1H-indol-1-yl)-2-hydroxy-2-methylpropanamide (18q). By Method A: To a solution of 4-fluoro-6-(4-fluoro-phenyl)-1H-indole (**16c**, 0.32 g, 1.4 mmol) in anhydrous THF (10 mL), which was cooled in an ice water bath under an argon atmosphere, was added sodium hydride (60% dispersion in oil, 0.17 g, 4.19 mmol). After addition, the resulting mixture was stirred for three hours. (S)-N-(4-Cyano-3-(trifluoromethyl)phenyl)-2-methyloxirane-2-carboxamide (**14**, 0.49 g, 1.40 mmol) was added to the above solution, and the resulting reaction mixture was allowed to stir overnight at room temperature under argon. The reaction was quenched by water, and extracted with ethyl acetate. The organic layer was washed with brine, dried with MgSO₄, filtered, and concentrated under vacuum. The product was purified by a silica gel column using ethyl acetate and hexanes (1:2, v/v) as eluent to afford 0.35 g (yield 50.5%) of the titled compound as off-white solid. ¹H NMR (400 MHz, DMSO-*d*₆) δ 10.30 (s, 1H, NH), 8.26 (d, *J* = 2.0 Hz, 1H, ArH), 8.07 (dd, *J* =

8.8 Hz, $J = 2.0$ Hz, 1H, ArH), 7.97 (d, $J = 8.8$ Hz, 1H, ArH), 7.68-7.64 (m, 2H, ArH), 7.60 (s, 1H, ArH), 7.35 (d, $J = 3.0$ Hz, 1H, ArH), 7.28-7.24 (m, 2H, ArH), 7.04 (dd, $J = 12.0$ Hz, 1.2 Hz, 1H, ArH), 6.48 (d, $J = 1.0$ Hz, 1H, ArH), 6.39 (s, 1H, OH), 4.67 (d, $J = 14.8$ Hz, 1H, CH), 4.42 (d, $J = 14.8$ Hz, 1H, CH), 1.49 (s, 3H, CH₃); MS (ESI, Negative) m/z [M - H]⁻; (ESI, Positive) 499.2056 [M + H]⁺.

(S)-N-(3-Chloro-4-cyanophenyl)-3-(3-fluoro-1H-indol-1-yl)-2-hydroxy-2-methylpropanamide (19a). By Method A: Yield 68%; Mp 168.9-170.1°C; Light brown solid; MS (ESI) m/z 369.8 [M - H]⁻; ¹H NMR (CDCl₃, 400 MHz) δ 8.66 (bs, 1H, NH), 7.81 (d, $J = 2.0$ Hz, 1H), 7.60-7.56 (m, 2H), 7.37 (dd, $J = 8.4, 2.0$ Hz, 2H), 7.23 (m, 1H), 7.12 (t, $J = 7.4$ Hz, 1H), 6.93 (d, $J = 2.8$ Hz, 1H), 4.56 (d, $J = 15.2$ Hz, 1H), 4.27 (d, $J = 15.2$ Hz, 1H), 2.44 (s, 1H, OH), 1.59 (s, 3H); ¹⁹F NMR (CDCl₃, decoupled) δ -173.91.

(S)-N-(3-Chloro-4-cyanophenyl)-3-(4-fluoro-1H-indol-1-yl)-2-hydroxy-2-methylpropanamide (19b). By Method A: Yield 73%; White solid; MS (ESI) m/z 369.9 [M - H]⁻; ¹H NMR (CDCl₃, 400 MHz) δ 8.64 (bs, 1H, NH), 7.81 (s, 1H), 7.57 (d, $J = 8.4$ Hz, 1H), 7.35 (d, $J = 7.2$ Hz, 1H), 7.21 (d, $J = 8.4$ Hz, 1H), 7.14-7.10 (m, 2H), 6.77 (t, $J = 8.4$ Hz, 1H), 6.63 (d, $J = 2.8$ Hz, 1H), 6.60 (s, 1H), 4.64 (d, $J = 14.8$ Hz, 1H), 4.35 (d, $J = 14.8$ Hz, 1H), 2.48 (bs, 1H, OH), 1.60 (s, 3H). ¹⁹F NMR (CDCl₃, decoupled) δ -121.78.

(S)-N-(3-Chloro-4-cyanophenyl)-3-(5-fluoro-1H-indol-1-yl)-2-hydroxy-2-methylpropanamide (19c). By Method A: Yield 79%; White solid; MS (ESI) m/z 371.0 [M - H]⁻; ¹H NMR (CDCl₃, 400 MHz) δ 8.62 (bs, 1H, NH), 7.80 (d, $J = 2.0$ Hz, 1H), 7.56 (d, $J = 8.4$ Hz, 1H), 7.38-7.34 (m, 2H), 7.23 (dd, $J = 9.2, 2.4$ Hz, 1H), 7.22 (dt, $J = 9.2, 2.8$ Hz, 1H), 7.15 (d, $J = 3.2$ Hz, 1H), 6.47 (d, $J = 3.2$ Hz, 1H), 4.63 (d, $J = 14.8$ Hz, 1H), 4.32 (d, $J = 14.8$ Hz, 1H), 2.49 (bs, 1H, OH), 1.60 (s, 3H); ¹⁹F NMR (CDCl₃, decoupled) δ -124.52.

(S)-N-(3-Chloro-4-cyanophenyl)-3-(6-fluoro-1H-indol-1-yl)-2-hydroxy-2-methylpropanamide (19d). By Method A: Yield 67%; White solid; MS (ESI) m/z 376.9 [M - H]⁻; ¹H NMR (CDCl₃, 400 MHz) δ 8.67 (bs, 1H, NH), 7.79 (d, J = 2.0 Hz, 1H), 7.56 (d, J = 8.4 Hz, 1H), 7.49 (dd, J = 8.4, 5.4 Hz, 1H), 7.38 (dd, J = 8.4, 2.0 Hz, 1H), 7.13 (dd, J = 10.0, 2.0 Hz, 1H), 7.09 (d, J = 3.2 Hz, 1H), 6.86 (m, 2H), 6.48 (d, J = 3.2 Hz, 1H), 4.58 (d, J = 14.8 Hz, 1H), 4.28 (d, J = 14.8 Hz, 1H), 2.61 (bs, 1H, OH), 1.60 (s, 3H); ¹⁹F NMR (CDCl₃, decoupled) δ -120.03.

(S)-N-(3-Chloro-4-cyanophenyl)-3-(7-fluoro-1H-indol-1-yl)-2-hydroxy-2-methylpropanamide (19e). By Method A: Yield 73%; White solid; MS (ESI) m/z 370.0 [M - H]⁻; ¹H NMR (CDCl₃, 400 MHz) δ 8.82 (d, J = 2.0 Hz, 1H), 8.60 (bs, 1H, NH), 7.55 (d, J = 8.4 Hz, 1H), 7.37-7.34 (m, 2H), 7.02 (d, J = 3.2 Hz, 1H), 7.00 (m, 1H), 7.01-6.98 (m, 1H), 6.91 (m, 1H), 6.46 (t, J = 2.8 Hz, 1H), 4.68 (d, J = 15.0 Hz, 1H), 4.62 (d, J = 15.0 Hz, 1H), 2.73 (d, J = 4.4 Hz, 1H, OH), 1.61 (s, 3H); ¹⁹F NMR (CDCl₃, decoupled) δ -133.54.

(S)-N-(3-Chloro-4-cyanophenyl)-3-(5-fluoro-6-phenyl-1H-indol-1-yl)-2-hydroxy-2-methylpropanamide (19f). By Method A: To a solution of 5-fluoro-6-phenyl-1H-indole (**16a**, 0.20 g, 0.947 mmol) in anhydrous THF (10 mL), which was cooled in an ice water bath under an argon atmosphere, was added sodium hydride (60% dispersion in oil, 0.076 g, 1.89 mmol). After addition, the resulting mixture was stirred for three hours. (*R*)-3-Bromo-*N*-(4-cyano-3-chlorophenyl)-2-hydroxy-2-methylpropanamide (**13**, 0.30 g, 0.947 mmol) was added to above solution, and the resulting reaction mixture was allowed to stir overnight at room temperature under argon. The reaction was quenched by water, and extracted with ethyl acetate. The organic layer was washed with brine, dried with MgSO₄, filtered, and concentrated under vacuum. The product was purified by a silica gel column using ethyl acetate and hexane (1:2, v/v) as eluent to afford

0.26 g of the titled compound as yellowish solid. Yield = 76%; ^1H NMR (400 MHz, $\text{DMSO-}d_6$) δ 10.11 (s, 1H, NH), 8.04 (d, $J = 1.6$ Hz, 1H, ArH), 7.80 (d, $J = 8.8$ Hz, 1H, ArH), 7.74 (dd, $J = 8.2$ Hz, $J = 2.0$ Hz, 1H, ArH), 7.62 (d, $J = 6.4$ Hz, 1H, ArH), 7.51-7.44 (m, 4H, ArH), 7.39-7.32 (m, 3H, ArH), 6.42 (d, $J = 3.2$ Hz, 1H, ArH), 6.33 (s, 1H, OH), 4.60 (d, $J = 15.2$ Hz, 1H, CH), 4.35 (d, $J = 15.2$ Hz, 1H, CH), 1.45 (s, 3H, CH_3). MS (ESI, Negative) m/z 445.8 $[\text{M} - \text{H}]^-$; (ESI, Positive) m/z 470.0 $[\text{M} + \text{Na}]^+$.

(S)-N-(3-Chloro-4-cyanophenyl)-3-(5-fluoro-3-phenyl-1H-indol-1-yl)-2-hydroxy-2-methylpropanamide (19g). By Method A: To a solution of 5-fluoro-3-phenyl-1H-indole (500 mg, 2.267 mmol) in anhydrous THF (10 mL), which was cooled in an ice water bath under an argon atmosphere, was added sodium hydride (60% dispersion in oil, 240 mg, 5.918 mmol). After addition, the resulting mixture was stirred for three hours. (*R*)-3-Bromo-*N*-(4-cyano-3-chloro-phenyl)-2-hydroxy-2-methylpropanamide (**13**, 0.75 g, 2.267 mmol) was added to the above solution, and the resulting reaction mixture was allowed to stir overnight at room temperature under argon. The reaction was quenched by water, and extracted with ethyl acetate. The organic layer was washed with brine, dried with MgSO_4 , filtered, and concentrated under vacuum. The product was purified by a silica gel column using ethyl acetate and hexane (1:2 to 1:1, v/v) as eluent to afford 0.43 g of the titled compound as yellowish solid. Yield = 85%; ^1H NMR (400 MHz, $\text{DMSO-}d_6$) δ 10.17 (s, 1H, NH), 8.06 (d, $J = 2.0$ Hz, 1H, ArH), 7.86-7.79 (m, 2H, ArH), 7.64 (s, 1H, ArH), 7.62-7.58 (m, 1H, ArH), 7.55-7.52 (m, 2H, ArH), 7.50 (dd, $J = 10.4$ Hz, $J = 2.4$ Hz, 1H, ArH), 7.43-7.40 (m, 2H, ArH), 7.26-7.22 (m, 1H, ArH), 7.03-6.98 (m, 1H, ArH), 6.37 (s, 1H, OH), 4.60 (d, $J = 14.8$ Hz, 1H, CH), 4.38 (d, $J = 14.8$ Hz, 1H, CH), 1.46 (s, 3H, CH_3). MS (ESI, Negative) m/z 446.8 $[\text{M} - \text{H}]^-$; (ESI, Positive) m/z 448.1248 $[\text{M} + \text{H}]^+$.

(S)-N-(4-Cyano-3-(trifluoromethyl)phenyl)-2-hydroxy-3-(indolin-1-yl)-2-methylpropanamide (20a). By Method B: Yield 71%; MS (ESI) 387.8 [M – H]⁻; ¹H NMR (400 MHz, CDCl₃) δ 9.24 (bs, 1H, NH), 8.09 (d, *J* = 2.0 Hz, 1H), 7.94 (dd, *J* = 8.4, 2.0 Hz, 1H), 7.78 (d, *J* = 8.4 Hz, 1H), 7.13-7.08 (m, 2H), 6.78 (d, *J* = 7.8, 0.8 Hz, 1H), 6.62 (d, *J* = 7.8, 0.8 Hz, 1H), 3.78 (s, 1H, OH), 3.66 (d, *J* = 14.4 Hz, 1H), 3.54 (t, *J* = 8.4 Hz, 1H), 3.46-3.40 (m, 1H), 3.32 (d, *J* = 14.4 Hz, 1H), 3.30 (m, 1H), 3.05-2.94 (m, 2H), 1.57 (s, 3H).

(S)-N-(4-Cyano-3-(trifluoromethyl)phenyl)-3-(4-fluoroindolin-1-yl)-2-hydroxy-2-methylpropanamide (20b). By Method B: Yield 75%; MS (ESI) *m/z* 406.0 [M – H]⁻; ¹H NMR (400 MHz, CDCl₃) δ 9.24 (bs, 1H, NH), 8.10 (d, *J* = 2.2 Hz, 1H), 7.95 (dd, *J* = 8.8, 2.2 Hz, 1H), 7.79 (d, *J* = 8.8 Hz, 1H), 6.83 (dd, *J* = 8.4, 2.4 Hz, 1H), 6.77 (m, 1H), 6.52 (dd, *J* = 8.4, 4.0 Hz, 1H), 3.75 (bs, 1H, OH), 3.64 (d, *J* = 14.0 Hz, 1H), 3.44 (m, 1H), 3.30 (q, *J* = 9.2 Hz, 1H), 3.22 (d, *J* = 14.0 Hz, 1H), 2.94 (m, 2H), 1.56 (s, 3H).

(S)-N-(4-Cyano-3-(trifluoromethyl)phenyl)-3-(6-fluoroindolin-1-yl)-2-hydroxy-2-methylpropanamide (20e). By Method B: Yield 47%; MS (ESI) *m/z* 405.9 [M – H]⁻; ¹H NMR (400 MHz, CDCl₃) δ 9.05 (bs, 1H, NH), 7.98 (d, *J* = 2.4 Hz, 1H), 7.62 (d, *J* = 8.4 Hz, 1H), 7.53 (dd, *J* = 8.4, 2.1 Hz, 1H), 7.04 (m, 1H), 6.48 (t, *J* = 8.4 Hz, 1H), 6.39 (d, *J* = 8.0 Hz, 1H), 3.68 (d, *J* = 14.4 Hz, 1H), 3.50 (bs, 1H, OH), 3.37 (q, *J* = 9.2 Hz, 1H), 3.29 (d, *J* = 14.02 Hz, 1H), 3.09 (m, 1H), 2.97 (m, 1H), 1.55 (s, 3H).

(S)-N-(4-Cyano-3-(trifluoromethyl)phenyl)-3-(5,6-difluoroindolin-1-yl)-2-hydroxy-2-methylpropanamide (20f). By Method B: Yield 59%; MS (ESI) *m/z* 424.07 [M – H]⁻; 426.06 [M + H]⁺; ¹H NMR (400 MHz, CDCl₃) δ 9.18 (bs, 1H, NH), 8.09 (d, *J* = 2.0 Hz, 1H), 7.97 (dd, *J* = 8.4, 2.0 Hz, 1H), 7.80 (d, *J* = 8.4 Hz, 1H), 6.89 (t, *J* = 8.8 Hz, 1H), 6.43 (m, 1H), 3.64 (d, *J* = 14.4 Hz, 1H), 3.46 (s, 1H, OH), 3.40-3.35 (m, 2H), 3.17 (d, *J* = 14.4 Hz, 1H), 2.99-2.91 (m, 2H),

1.57 (s, 3H), ¹⁹F NMR (CDCl₃, decoupled) δ -62.21 (CF₃), -139.18 (d, *J*_{F-F} = -21.6 Hz, Ar-F), -150.28 (d, *J*_{F-F} = -21.6 Hz, Ar-F).

(S)-3-(5-Chloro-6-fluoroindolin-1-yl)-N-(4-cyano-3-(trifluoromethyl)phenyl)-2-hydroxy-2-methylpropanamide (20g). By Method B: Yield 47%; MS (ESI) *m/z* 440.3 [M – H][–]; ¹H NMR (400 MHz, CDCl₃) δ 9.15 (bs, 1H, NH), 8.02 (d, *J* = 8.4 Hz, 1H), 7.81 (d, *J* = 8.4 Hz, 1H), 7.03 (d, *J* = 7.2 Hz, 1H), 6.42 (d, *J* = 10.0 Hz, 1H), 3.66 (d, *J* = 14.4 Hz, 1H), 3.52-3.42 (m, 2H), 3.38 (s, 1H, OH), 3.21 (d, *J* = 14.4 Hz, 1H), 2.96-2.80 (m, 2H), 1.52 (s, 3H).

(S)-N-(3-Chloro-4-cyanophenyl)-3-(4-fluoroindolin-1-yl)-2-hydroxy-2-methylpropanamide (21a). By Method B: Yield 71%; MS (ESI) *m/z* 372.0 [M – H][–]; [α]_D²⁰ = 173° (*c* 1.0, CH₃OH); ¹H NMR (400 MHz, CDCl₃) δ 9.05 (bs, 1H, NH), 7.98 (d, *J* = 2.4 Hz, 1H), 7.62 (d, *J* = 8.4 Hz, 1H), 7.53 (dd, *J* = 8.4, 2.1 Hz, 1H), 7.04 (m, 1H), 6.48 (t, *J* = 8.4 Hz, 1H), 6.39 (d, *J* = 8.0 Hz, 1H), 3.68 (d, *J* = 14.4 Hz, 1H), 3.50 (bs, 1H, OH), 3.37 (q, *J* = 9.2 Hz, 1H), 3.29 (d, *J* = 14.2 Hz, 1H), 3.09 (m, 1H), 2.97 (m, 1H), 1.55 (s, 3H).

(S)-N-(3-Chloro-4-cyanophenyl)-3-(5-fluoroindolin-1-yl)-2-hydroxy-2-methylpropanamide (21b). By Method B: Yield 64%; MS (ESI) *m/z* 372.0 [M – H][–]; [α]_D²⁰ = -202°; ¹H NMR (400 MHz, CDCl₃) δ 9.05 (bs, 1H, NH), 7.98 (d, *J* = 2.4 Hz, 1H), 7.62 (d, *J* = 8.4 Hz, 1H), 7.53 (dd, *J* = 8.4, 2.1 Hz, 1H), 7.04 (m, 1H), 6.48 (t, *J* = 8.4 Hz, 1H), 6.39 (d, *J* = 8.0 Hz, 1H), 3.68 (d, *J* = 14.4 Hz, 1H), 3.50 (bs, 1H, OH), 3.37 (q, *J* = 9.2 Hz, 1H), 3.29 (d, *J* = 14.2 Hz, 1H), 3.09 (m, 1H), 2.97 (m, 1H), 1.55 (s, 3H).

(S)-3-(5-Bromoindolin-1-yl)-N-(3-chloro-4-cyanophenyl)-2-hydroxy-2-methylpropanamide (21c). By Method B: Yield 54%; MS (ESI) *m/z* 433.6 [M – H][–]; ¹H NMR (400 MHz, CDCl₃) δ 9.04 (bs, 1H, NH), 7.98 (d, *J* = 2.0 Hz, 1H), 7.60 (d, *J* = 6.0 Hz, 1H), 7.52 (dd, *J* = 6.0, 2.0 Hz, 1H), 7.19-7.17 (m, 2H), 6.49 (d, *J* = 8.4 Hz, 1H), 3.65 (d, *J* = 14.4, 1H),

3.47 (bs, 1H, OH), 3.36-3.41 (m, 1H), 3.32 (q, $J = 9.2$ Hz, 1H), 3.23 (d, $J = 14.4$, 1H), 2.99-2.91 (m, 2H), 1.56 (s, 3H).

(S)-N-(3-Chloro-4-cyanophenyl)-3-(6-fluoroindolin-1-yl)-2-hydroxy-2-methylpropanamide (21d). By Method B: Yield 68%; MS (ESI) m/z 372.1 $[M - H]^-$; 396.3 $[M + Na]^+$; 1H NMR (400 MHz, $CDCl_3$) δ 9.08 (bs, 1H, NH), 7.98 (d, $J = 1.6$ Hz, 1H), 7.60 (d, $J = 8.6$ Hz, 1H), 7.54 (dd, $J = 8.6, 1.6$ Hz, 1H), 6.98 (t, $J = 6.4$ Hz, 1H), 6.40 (m, 1H), 6.38 (d, $J = 10.0$ Hz, 1H), 3.65 (d, $J = 14.4$ Hz, 1H), 3.51 (bs, 1H, OH), 3.50-3.45 (m, 1H), 3.40 (q, $J = 9.2$ Hz, 1H), 3.23 (d, $J = 14.2$ Hz, 1H), 3.00-2.87 (m, 2H), 1.56 (s, 3H).

(S)-N-(3-Chloro-4-cyanophenyl)-3-(5,6-difluoroindolin-1-yl)-2-hydroxy-2-methylpropanamide (21e). By Method B: Yield 64%; MS (ESI) m/z 390.0 $[M - H]^-$; 1H NMR (400 MHz, $CDCl_3$) δ 9.05 (bs, 1H, NH), 7.98 (s, 1H), 7.62 (d, $J = 8.2$ Hz, 1H), 7.53 (d, $J = 8.2$ Hz, 1H), 6.88 (t, $J = 8.8$ Hz, 1H), 6.43 (m, 1H), 3.95-3.88 (m, 2H), 3.64 (d, $J = 14.4$ Hz, 1H), 3.46 (s, 1H, OH), 3.44 (m, 1H), 3.42-3.34 (m, 1H), 3.16 (d, $J = 14.4$ Hz, 1H), 1.55 (s, 3H).

(S)-N-(3-Chloro-4-cyanophenyl)-3-(5-fluoro-6-phenylindolin-1-yl)-2-hydroxy-2-methylpropanamide (21f). To a solution of compound **19f** (185 mg, 0.413 mmol) in 5 mL of glacial acetic acid which was cooled in an ice-water bath, was added dropwise sodium cyanoborohydride (1.0 M in THF, 0.62 mL, 1.24 mmol) under an argon atmosphere. After addition, the resulting reaction mixture was allowed to stir for overnight at room temperature under argon. The reaction was quenched by aqueous NH_4Cl solution, and extracted with ethyl acetate. The organic layer was washed with brine twice, dried with $MgSO_4$, filtered, and concentrated under vacuum. The product was purified by a silica gel column using ethyl acetate and hexane (1:2, v/v) as eluent to afford 0.17 g of the titled compound as yellowish foam. Yield = 42%; 1H NMR (400 MHz, $DMSO-d_6$) δ 10.29 (s, 1H, NH), 8.21 (d, $J = 2.0$ Hz, 1H, ArH),

7.92-7.84 (m, 2H, ArH), 7.45-7.34 (m, 5H, ArH), 6.95 (d, $J = 10.4$ Hz, 1H, ArH), 6.55 (d, $J = 6.4$ Hz, 1H, ArH), 6.02 (s, 1H, OH), 4.50 (d, $J = 14.4$ Hz, 1H, CH), 4.19 (d, $J = 14.4$ Hz, 1H, CH), 3.61 (q, $J = 8.8$ Hz, 1H, CH), 3.40 (d, $J = 14.4$ Hz, 1H, CH), 2.91 (t, $J = 8.4$ Hz, 2H, CH₂), 1.42 (s, 3H, CH₃); MS (ESI, Positive) m/z 450.1394 [M + H]⁺.

Biological Experiments: Plasmid constructs and transient transfection. GRE-LUC, CMV-renilla LUC, and CMV-hAR, used for the transient transfection assays were described earlier.²⁸ Transient transactivation studies were performed in HEK-293 or COS cells using Lipofectamine as described before. Briefly, cells were plated in 24-well plates at 70,000 cells/well in Dulbecco's Medium Eagle plus 5% charcoal-stripped fetal bovine serum (csFBS) without phenol red. Twenty four hours after plating, the cells were transfected with 0.25 μ g GRE-LUC, 10 ng CMV-LUC, and 25 ng CMV-hAR using Lipofectamine in OptiMEM medium. Cells were treated 24 h after transfection with a dose response of antagonists in combination with 0.1 nM R1881 (i.e., antagonist mode) and luciferase assay was performed 48 h after transfection. Firefly luciferase values were normalized to renilla luciferase values. Agonist mode experiments were run in some cases and were similar to antagonist mode except the dose response was the agonist in question without any antagonist nor co-treatment with R1881.

Competitive ligand binding assay. A ligand binding assay with purified GST-tagged AR-LBD and 1 nM ³H-mibolerone was performed as described previously.²⁸ Purified AR protein was incubated with 1 nM ³H-mibolerone, a dose response of SARs (1 pM to 100 μ M) or DHT (used as control in all experiments) for 16 h at 4 °C. The protein complex was precipitated using hydroxyapatite (Bio-Rad, Hercules, CA), washed 4-6 times, and the bound radioactivity was eluted using 100% ethanol. The eluted tritium was counted using a scintillation

counter. The inhibitory constant (K_i) was obtained from modeling the data using SigmaPlot® software. The values are expressed as relative to DHT with DHT taken as 1 nM.

Western blotting. Cells were plated at 1-1.5 million cells per well in 6-well plates or in 60 mm plates in RPMI + 1% csFBS containing medium and treated as described in the respective figures. Protein extracts were prepared 24 h after treatment, fractionated with SDS polyacrylamide gel electrophoresis (SDS-PAGE), and Western blot was performed using respective antibodies as described previously.²⁸ Experiments with the proteasome inhibitor bortezomib were conducted in MR49F cells plated in growth medium and treated with 10 μ M bortezomib alone or in combination with 10 μ M of **19b** or **19f**. Cells were simultaneously treated with 50 μ M cycloheximide. Cells were harvested 8 hours after treatment and Western blot for AR and GAPDH was performed.

Proliferation assay. Cells were plated in charcoal-stripped FBS-containing medium in 96 well plates. Cells were treated with the indicated doses of the compound. Three days after the initial treatment, cells were re-treated in fresh medium. Six days after treatment cells were fixed and stained with sulforhodamine B dye and the number of viable cells was measured at O.D. 535 nm.

Metabolic stability in mouse liver microsomes. Test compound stock solutions were prepared at 10 mM in DMSO. They were diluted to a concentration of 50 μ M in 50% ACN/H₂O resulting in a working stock solution of 100 X. Liver microsomes were utilized at a final concentration of 1.0 mg/mL of protein. Duplicate wells were used for each time point (0, 5, 10, 30, and 60 minutes).

Cofactors were added for phase II. Reactions were carried out at 37°C in a shaking water bath, and the final concentration of solvent was kept constant at 0.5%. At each time point, 100 µL of reaction was removed and added to a sample well containing 100 µL of ice-cold, 100% ACN (plus internal standard), to stop the reaction. The final volume for each reaction was 200 µL, composed of: 66 µL of 0.2 M KPO₄ buffer, (pH 7.4); 50 µL of NRS solution; and 10 µL of microsomes (20 mg/ml stock). The NRS is a solution of glucose-6-phosphate dehydrogenase, NADP⁺, MgCl₂, and glucose-6-phosphate, prepared per manufacturer's instructions. Each 5.0 mL stock of NRS solution contains 3.8 mL H₂O, 1.0 mL solution "A", and 0.2 mL solution "B". Reactions from the positive control wells (verapamil, 0.5 µM) were stopped with ice cold ACN containing internal standard.

Fluorescence polarization. Fluorescence polarization studies to determine the binding of the SARDs to AF-1 domain of the AR was conducted as published earlier.²⁸

Xenograft studies. All animal protocols were approved by the University of Tennessee Health Science Center Animal Care and Use Committee. Male NSG mice (6-8 weeks old) purchased from JAX labs (Bar Harbor, ME) were housed as five animals per cage and were allowed free access to water and commercial rodent chow (Harlan Teklad 22/5 rodent diet - 8640). Cell line xenografts were performed as previously published.²⁸ Enz-R LNCaP cells (i.e., MR49F cells, a kind gift from Dr. Martin Gleeve, University of British Columbia) (5 million) grown in growth medium were mixed with Matrigel (BD Biosciences, San Jose, CA) at 1:1 ratio and injected subcutaneously in NSG mice. Once tumor sizes reached 100-200 mm³, the animals were castrated and the tumors were allowed to regrow as CRPC. The animals were randomized once the tumors started to regrow and treated with vehicle (polyethylene glycol-300: DMSO 85:15 ratio) or SARDs orally. Tumor volume was calculated using the formula

length*width*width*0.5236. At the end of the experiments, animals were sacrificed, tumors were weighed and collected for further processing.

Hershberger assay. Male C57B/L6 mice or Sprague Dawley rats were treated as indicated in the figures. Fourteen days after treatment, the animals were sacrificed and the weights of androgen-dependent tissues, prostate and seminal vesicles were recorded and represented as percent change from vehicle-treated animals. As prostate is too small to precisely excise from mice, only seminal vesicles were obtained and reported.

Ancillary Information.

Supporting Information.

The Supporting Information is available free of charge on the ACS Publications website.

Additional information on compound characterization; additional biological experiments and figures (PDF)

Molecular formula strings (CSV)

Corresponding Author

*D.D.M.: Phone: +1-901-448-6026. Fax: +1-901-448-3446. E-mail: dmiller@uthsc.edu.

ORCID ID

Dong-Jin Hwang: 0000-0002-0055-1916

Yali He: 0000-0002-4431-6723

Suriyan Ponnusamy: 0000-0001-8257-3993

Michael L. Mohler: 0000-0002-1609-6524

Thirumagal Thiyagarajan: 0000-0002-7813-0556

Iain J. McEwan: 0000-0003-2087-0663

Ramesh Narayanan: 0000-0001-5490-0790

Duane D. Miller: 0000-0002-6903-9085

Author Contributions.

The manuscript was written through contributions of all authors. All authors have given approval to the final version of the manuscript.

Acknowledgments.

This research was supported by the Van Vleet Endowed Professorship (D.D.M.), and GTx, Inc. grant (R.N. and D.D.M.) We thank GTx, Inc. for supporting this project and Dr. Dejian Ma of UTHSC, College of Pharmacy for assistance with 2D NMR and HRMS experiments.

ABBREVIATIONS USED.

PC: prostate cancer, SARs: selective androgen receptor degraders, AR: androgen receptor, SV: splice variant, ADT: androgen deprivation therapy, DHT: 5 α -dihydrotestosterone, CRPC: castration-resistant prostate cancer, LBD: ligand binding domain, FL: full length, Enz-R: enzalutamide resistant, SAR: structure activity relationship, SARM: selective androgen receptor modulator, GR: glucocorticoid receptor, ER: estrogen receptor, PR: progesterone receptor, DMPK: drug metabolism and pharmacokinetics, MLM: mouse liver microsomes, RLU: relative light units, MIB: milbolerone, NTD: N-terminal domain, PROTACs: proteolysis-targeting chimaeras, csFBS:

charcoal-stripped fetal bovine serum, EWG: electron withdrawing group, GRE: glucocorticoid response element, NSG: NOD SCID gamma, TGI: tumor growth inhibition.

Notes: R.N. is a consultant to GTx, Inc. The authors, except I.J.M, M.L.M. and T.T., own intellectual property rights to the molecules described in this manuscript. The molecules have been exclusively licensed to GTx, Inc., Memphis, TN.

\

References

- (1) Ban, F.; Leblanc, E.; Li, H.; Munuganti, R. S.; Frewin, K.; Rennie, P. S.; Cherkasov, A. Discovery of 1*H*-indole-2-carboxamides as novel inhibitors of the androgen receptor binding function 3 (BF3). *J. Med. Chem.* **2014**, *57* (15), 6867-6872.
- (2) Huggins, C. H.; Hodges, C. V. Studies on prostatic cancer, I: the effect of castration, of estrogen and of androgen injection on serum phosphatases in metastatic carcinoma of the prostate. *Cancer Research* **1941**, *1*, 293-297.
- (3) Schmidt, L. J.; Tindall, D. J. Androgen receptor: past, present and future. *Curr. Drug Targets* **2013**, *14* (4), 401-407.
- (4) Siegel, R. L.; Miller, K. D.; Jemal, A. Cancer statistics, 2018. *CA Cancer J. Clin.* **2018**, *68* (1), 7-30.
- (5) Torre, L. A.; Bray, F.; Siegel, R. L.; Ferlay, J.; Lortet-Tieulent, J.; Jemal, A. Global cancer statistics, 2012. *CA Cancer J. Clin.* **2015**, *65* (2), 87-108.
- (6) Huang, H.; Tindall, D. J. The role of the androgen receptor in prostate cancer. *Crit. Rev. Eukaryot. Gene Expr.* **2002**, *12* (3), 193-207.
- (7) Koochekpour, S. Androgen receptor signaling and mutations in prostate cancer. *Asian J. Androl.* **2010**, *12* (5), 639-657.
- (8) Fujimoto, N. Role of the androgen-androgen receptor axis in the treatment resistance of advanced prostate cancer: from androgen-dependent to castration resistant and further. *J. UOEH* **2016**, *38* (2), 129-138.
- (9) Mohler, J. L.; Gregory, C. W.; Ford, O. H., 3rd; Kim, D.; Weaver, C. M.; Petrusz, P.; Wilson, E. M.; French, F. S. The androgen axis in recurrent prostate cancer. *Clin. Cancer Res.* **2004**, *10* (2), 440-448.

- (10) Mout, L.; de Wit, R.; Stuurman, D.; Verhoef, E.; Mathijssen, R.; de Ridder, C.; Lolkema, M.; van Weerden, W. Testosterone diminishes cabazitaxel efficacy and intratumoral accumulation in a prostate cancer xenograft model. *EBioMedicine* **2018**, *27*, 182-186.
- (11) Scher, H. I.; Fizazi, K.; Saad, F.; Taplin, M. E.; Sternberg, C. N.; Miller, K.; de Wit, R.; Mulders, P.; Chi, K. N.; Shore, N. D.; Armstrong, A. J.; Flaig, T. W.; Flechon, A.; Mainwaring, P.; Fleming, M.; Hainsworth, J. D.; Hirmand, M.; Selby, B.; Seely, L.; de Bono, J. S. Investigators, A. Increased survival with enzalutamide in prostate cancer after chemotherapy. *N. Engl. J. Med.* **2012**, *367* (13), 1187-1197.
- (12) Chong, J. T.; Oh, W. K.; Liaw, B. C. Profile of apalutamide in the treatment of metastatic castration-resistant prostate cancer: evidence to date. *Onco. Targets Ther.* **2018**, *11*, 2141-2147.
- (13) Smith, M. R.; Saad, F.; Chowdhury, S.; Oudard, S.; Hadaschik, B. A.; Graff, J. N.; Olmos, D.; Mainwaring, P. N.; Lee, J. Y.; Uemura, H.; Lopez-Gitlitz, A.; Trudel, G. C.; Espina, B. M.; Shu, Y.; Park, Y. C.; Rackoff, W. R.; Yu, M. K.; Small, E. J.; Investigators, S. Apalutamide treatment and metastasis-free survival in prostate cancer. *N. Engl. J. Med.* **2018**, *378* (15), 1408-1418.
- (14) Korpai, M.; Korn, J. M.; Gao, X.; Rakiec, D. P.; Ruddy, D. A.; Doshi, S.; Yuan, J.; Kovats, S. G.; Kim, S.; Cooke, V. G.; Monahan, J. E.; Stegmeier, F.; Roberts, T. M.; Sellers, W. R.; Zhou, W.; Zhu, P. An F876L mutation in androgen receptor confers genetic and phenotypic resistance to MDV3100 (enzalutamide). *Cancer Discov.* **2013**, *3* (9), 1030-1043.
- (15) Kurmis, A. A.; Yang, F.; Welch, T. R.; Nickols, N. G.; Dervan, P. B. A pyrrole-imidazole polyamide is active against enzalutamide-resistant prostate cancer. *Cancer Res.* **2017**, *77* (9), 2207-2212.

- (16) Ge, R.; Xu, X.; Xu, P.; Li, L.; Li, Z.; Bian, J. Degradation of androgen receptor through small molecules for prostate cancer. *Curr. Cancer Drug Targets* **2018**, *18* (7), 652-667.
- (17) Attard, G.; Borre, M.; Gurney, H.; Lortol, Y.; Andresen-Daniil, C.; Kalleda, R.; Pham, T.; Taplin, M. E. Abiraterone alone or in combination with enzalutamide in metastatic castration-resistant prostate cancer with rising prostate-specific antigen during enzalutamide treatment. *J. Clin. Oncol.* **2018**, *36* (25), 2639–2646.
- (18) Culig, Z. Molecular mechanisms of enzalutamide resistance in prostate cancer. *Curr. Mol. Biol. Rep.* **2017**, *3* (4), 230-235.
- (19) Lombard, A. P.; Liu, L.; Cucchiara, V.; Liu, C.; Armstrong, C. M.; Zhao, R.; Yang, J. C.; Lou, W.; Evans, C. P.; Gao, A. C. Intra vs inter cross-resistance determines treatment sequence between taxane and AR-targeting therapies in advanced prostate cancer. *Mol. Cancer Ther.* **2018**, *17* (10), 2197–2205.
- (20) Hornberg, E.; Ylitalo, E. B.; Crnalic, S.; Antti, H.; Stattin, P.; Widmark, A.; Bergh, A.; Wikstrom, P. Expression of androgen receptor splice variants in prostate cancer bone metastases is associated with castration-resistance and short survival. *PLoS One* **2011**, *6* (4), e19059.
- (21) Seitz, A. K.; Thoene, S.; Bietenbeck, A.; Nawroth, R.; Tauber, R.; Thalgott, M.; Schmid, S.; Secci, R.; Retz, M.; Gschwend, J. E.; Ruland, J.; Winter, C.; Heck, M. M., AR-V7 in peripheral whole blood of patients with castration-resistant prostate cancer: Association with treatment-specific outcome under abiraterone and enzalutamide. *Eur. Urol.* **2017**, *72* (5), 828-834.
- (22) Joseph, J. D.; Lu, N.; Qian, J.; Sensintaffar, J.; Shao, G.; Brigham, D.; Moon, M.; Maneval, E. C.; Chen, I.; Darimont, B.; Hager, J. H. A clinically relevant androgen receptor

mutation confers resistance to second-generation antiandrogens enzalutamide and ARN-509.

Cancer Discov. **2013**, *3* (9), 1020-1029.

(23) Hara, T.; Miyazaki, J.; Araki, H.; Yamaoka, M.; Kanzaki, N.; Kusaka, M.; Miyamoto, M.

Novel mutations of androgen receptor: a possible mechanism of bicalutamide withdrawal syndrome. *Cancer Res.* **2003**, *63* (1), 149-153.

(24) Marques, R. B.; Erkens-Schulze, S.; de Ridder, C. M.; Hermans, K. G.; Waltering, K.; Visakorpi, T.; Trapman, J.; Romijn, J. C.; van Weerden, W. M.; Jenster, G. Androgen receptor modifications in prostate cancer cells upon long-term androgen ablation and antiandrogen treatment. *Int. J. Cancer* **2005**, *117* (2), 221-229.

(25) Bohl, C. E.; Gao, W.; Miller, D. D.; Bell, C. E.; Dalton, J. T. Structural basis for antagonism and resistance of bicalutamide in prostate cancer. *Proc. Natl. Acad. Sci. U S A* **2005**, *102* (17), 6201-6206.

(26) Dalton, J. T.; Mukherjee, A.; Zhu, Z.; Kirkovsky, L.; Miller, D. D. Discovery of nonsteroidal androgens. *Biochem Biophys Res Commun* **1998**, *244* (1), 1-4.

(27) Hwang, D. J.; Yang, J.; Xu, H.; Rakov, I. M.; Mohler, M. L.; Dalton, J. T.; Miller, D. D., Arylisothiocyanato selective androgen receptor modulators (SARMs) for prostate cancer. *Bioorg. Med. Chem.* **2006**, *14* (19), 6525-6538.

(28) Ponnusamy, S.; Coss, C. C.; Thiyagarajan, T.; Watts, K.; Hwang, D. J.; He, Y.; Selth, L. A.; McEwan, I. J.; Duke, C. B.; Pagadala, J.; Singh, G.; Wake, R. W.; Ledbetter, C.; Tilley, W. D.; Moldoveanu, T.; Dalton, J. T.; Miller, D. D.; Narayanan, R. Novel selective agents for the degradation of androgen receptor variants to treat castration-resistant prostate cancer. *Cancer Res.* **2017**, *77* (22), 6282-6298.

- (29) Bohl, C. E.; Wu, Z.; Miller, D. D.; Bell, C. E.; Dalton, J. T. Crystal structure of the T877A human androgen receptor ligand-binding domain complexed to cyproterone acetate provides insight for ligand-induced conformational changes and structure-based drug design. *J. Biol. Chem.* **2007**, *282* (18), 13648-13655.
- (30) Chen, J.; Hwang, D. J.; Chung, K.; Bohl, C. E.; Fisher, S. J.; Miller, D. D.; Dalton, J. T. In vitro and in vivo structure-activity relationships of novel androgen receptor ligands with multiple substituents in the B-ring. *Endocrinology* **2005**, *146* (12), 5444-5454.
- (31) Gao, W.; Bohl, C. E.; Dalton, J. T. Chemistry and structural biology of androgen receptor. *Chem. Rev.* **2005**, *105* (9), 3352-3370.
- (32) Gao, W.; Wu, Z.; Bohl, C. E.; Yang, J.; Miller, D. D.; Dalton, J. T. Characterization of the in vitro metabolism of selective androgen receptor modulator using human, rat, and dog liver enzyme preparations. *Drug Metab. Dispos.* **2006**, *34* (2), 243-253.
- (33) Jones, A.; Chen, J.; Hwang, D. J.; Miller, D. D.; Dalton, J. T. Preclinical characterization of a (*S*)-*N*-(4-cyano-3-trifluoromethyl-phenyl)-3-(3-fluoro, 4-chlorophenoxy)-2-hydroxy-2-methyl-propanamide: a selective androgen receptor modulator for hormonal male contraception. *Endocrinology* **2009**, *150* (1), 385-395.
- (34) Jones, A.; Hwang, D. J.; Duke, C. B., 3rd; He, Y.; Siddam, A.; Miller, D. D.; Dalton, J. T., Nonsteroidal selective androgen receptor modulators enhance female sexual motivation. *J. Pharmacol. Exp. Ther.* **2010**, *334* (2), 439-448.
- (35) Jones, A.; Hwang, D. J.; Narayanan, R.; Miller, D. D.; Dalton, J. T. Effects of a novel selective androgen receptor modulator on dexamethasone-induced and hypogonadism-induced muscle atrophy. *Endocrinology* **2010**, *151* (8), 3706-3719.

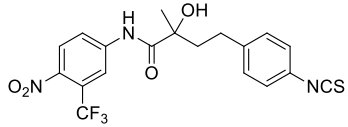
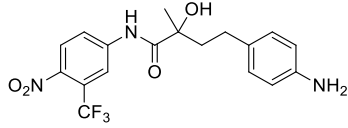
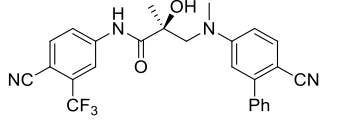
- (36) Kim, J.; Wu, D.; Hwang, D. J.; Miller, D. D.; Dalton, J. T. The para substituent of S-3-(phenoxy)-2-hydroxy-2-methyl-N-(4-nitro-3-trifluoromethyl-phenyl)-propionamides is a major structural determinant of in vivo disposition and activity of selective androgen receptor modulators. *J. Pharmacol. Exp. Ther.* **2005**, *315* (1), 230-239.
- (37) Li, W.; Hwang, D. J.; Cremer, D.; Joo, H.; Kraka, E.; Kim, J.; Ross, C. R., 2nd; Nguyen, V. Q.; Dalton, J. T.; Miller, D. D. Structure determination of chiral sulfoxide in diastereomeric bicalutamide derivatives. *Chirality* **2009**, *21* (6), 578-583.
- (38) Mohler, M. L.; Coss, C. C.; Duke, C. B., 3rd; Patil, S. A.; Miller, D. D.; Dalton, J. T. Androgen receptor antagonists: a patent review (2008-2011). *Expert Opin Ther Pat.* **2012**, *22* (5), 541-565.
- (39) Mohler, M. L.; He, Y.; Hwang, D. J.; Bohl, C. E.; Narayanan, R.; Dalton, J. T.; Miller, D. D. *Nonsteroidal Tissue Selective Androgen Receptor Modulators in Nuclear Receptors as Drug Targets*. Wiley-VCH: Weinheim: 2008.
- (40) Mohler, M. L.; Nair, V. A.; Hwang, D. J.; Rakov, I. M.; Patil, R.; Miller, D. D. Nonsteroidal tissue selective androgen receptor modulators: A promising class of clinical candidates. *Expert Opin Ther Pat.* **2005**, *15* (11), 1565-1585.
- (41) Narayanan, R.; Coss, C. C.; Yepuru, M.; Kearbey, J. D.; Miller, D. D.; Dalton, J. T. Steroidal androgens and nonsteroidal, tissue-selective androgen receptor modulator, S-22, regulate androgen receptor function through distinct genomic and nongenomic signaling pathways. *Mol. Endocrinol.* **2008**, *22* (11), 2448-2465.
- (42) Yang, J.; Ahn, S.; Wu, Z.; Hwang, D. J.; Miller, D. D.; Dalton, J. T. Pharmacokinetics, pharmacodynamics and metabolism of a novel anticancer agent for prostate cancer. *Int J Oncol* **2012**, *41* (1), 337-344.

- (43) Coss, C. C.; Jones, A.; Dalton, J. T. Pharmacokinetic drug interactions of the selective androgen receptor modulator GTx-024 (Enobosarm) with itraconazole, rifampin, probenecid, celecoxib and rosuvastatin. *Invest New Drugs* **2016**, *34* (4), 458-467.
- (44) Ponnusamy, S.; Sullivan, R. D.; Thiyagarajan, T.; Tillmann, H.; Getzenberg, R. H.; Narayanan, R. Tissue Selective Androgen Receptor Modulators (SARMs) increase pelvic floor muscle mass in ovariectomized mice. *J. Cell Biochem.* **2017**, *118* (3), 640-646.
- (45) Lipinski, C. A.; Lombardo, F.; Dominy, B. W.; Feeney, P. J., Experimental and computational approaches to estimate solubility and permeability in drug discovery and development settings. *Adv. Drug Deliv. Rev.* **2001**, *46* (1-3), 3-26.
- (46) Nair, V. A.; Mustafa, S. M.; Mohler, M. L.; Fisher, S. J.; Dalton, J. D.; Miller, D. D. Synthesis of novel iodo derivated bicalutamide analogs. *Tetrahedron letters* **2005**, *45* (51), 9475-9477.
- (47) Bohl, C. E.; Wu, Z.; Chen, J.; Mohler, M. L.; Yang, J.; Hwang, D. J.; Mustafa, S.; Miller, D. D.; Bell, C. E.; Dalton, J. T. Effect of B-ring substitution pattern on binding mode of propionamide selective androgen receptor modulators. *Bioorg. Med. Chem. Lett.* **2008**, *18* (20), 5567-5570.
- (48) Chen, J.; Hwang, D. J.; Bohl, C. E.; Miller, D. D.; Dalton, J. T. A selective androgen receptor modulator for hormonal male contraception. *J. Pharmacol. Exp. Ther.* **2005**, *312* (2), 546-553.
- (49) Kirkovsky, L.; Mukherjee, A.; Yin, D.; Dalton, J. T.; Miller, D. D. Chiral nonsteroidal affinity ligands for the androgen receptor. 1. Bicalutamide analogues bearing electrophilic groups in the B aromatic ring. *J. Med. Chem.* **2000**, *43* (4), 581-590.

- (50) Munuganti, R. S.; Hassona, M. D.; Leblanc, E.; Frewin, K.; Singh, K.; Ma, D.; Ban, F.; Hsing, M.; Adomat, H.; Lallous, N.; Andre, C.; Jonadass, J. P.; Zoubeydi, A.; Young, R. N.; Guns, E. T.; Rennie, P. S.; Cherkasov, A. Identification of a potent antiandrogen that targets the BF3 site of the androgen receptor and inhibits enzalutamide-resistant prostate cancer. *Chem. Biol.* **2014**, *21* (11), 1476-1485.
- (51) Clegg, N. J.; Wongvipat, J.; Joseph, J. D.; Tran, C.; Ouk, S.; Dilhas, A.; Chen, Y.; Grillot, K.; Bischoff, E. D.; Cai, L.; Aparicio, A.; Dorow, S.; Arora, V.; Shao, G.; Qian, J.; Zhao, H.; Yang, G.; Cao, C.; Sensintaffar, J.; Wasielewska, T.; Herbert, M. R.; Bonnefous, C.; Darimont, B.; Scher, H. I.; Smith-Jones, P.; Klang, M.; Smith, N. D.; De Stanchina, E.; Wu, N.; Ouerfelli, O.; Rix, P. J.; Heyman, R. A.; Jung, M. E.; Sawyers, C. L.; Hager, J. H. ARN-509: a novel antiandrogen for prostate cancer treatment. *Cancer Res.* **2012**, *72* (6), 1494-1503.
- (52) Liu, H. L.; Zhong, H. Y.; Song, T. Q.; Li, J. Z., A Molecular modeling study of the hydroxyflutamide resistance mechanism induced by androgen receptor mutations. *Int. J. Mol. Sci.* **2017**, *18* (9), e1823.
- (53) Attardi, B. J.; Burgenson, J.; Hild, S. A.; Reel, J. R., Steroid hormonal regulation of growth, prostate specific antigen secretion, and transcription mediated by the mutated androgen receptor in CWR22Rv1 human prostate carcinoma cells. *Mol. Cell Endocrinol.* **2004**, *222* (1-2), 121-132.
- (54) Hörnberg, E.; Ylitalo, E. B.; Crnalic, S.; Antti, H.; Stattin, P.; Widmark, A.; Bergh, A.; Wikstrom, P. Expression of androgen receptor splice variants in prostate cancer bone metastases is associated with castration-resistance and short survival. *PLoS One* **2011**, *6* (4), e19059

- (55) Wu, H.; Zhang, L.; Gao, X.; Zhang, X.; Duan, J.; You, L.; Cheng, Y.; Bian, J.; Zhu, Q.; Yang, Y. Combination of sorafenib and enzalutamide as a potential new approach for the treatment of castration-resistant prostate cancer. *Cancer Lett.* **2017**, *385*, 108-116.
- (56) Stice, J. P.; Wardell, S. E.; Norris, J. D.; Yllanes, A. P.; Alley, H. M.; Haney, V. O.; White, H. S.; Safi, R.; Winter, P. S.; Cocce, K. J.; Kishton, R. J.; Lawrence, S. A.; Strum, J. C.; McDonnell, D. P. CDK4/6 therapeutic intervention and viable alternative to taxanes in CRPC. *Mol. Cancer Res.* **2017**, *15* (6), 660-669.
- (57) Crews, C. M. Inducing protein degradation as a therapeutic strategy. *J. Med. Chem.* **2018**, *61*, 403–404.
- (58) Ge, R.; Xu, X.; Xu, P.; Li, L.; Li, Z.; Bian, J. Degradation of androgen receptor through small molecules for prostate cancer. *Current Cancer Drug Targets* **2018**, *17* (16), 652-667.
- (59) Lin, S. J.; Chou, F. J.; Li, L.; Lin, C. Y.; Yeh, S.; Chang, C. Natural killer cells suppress enzalutamide resistance and cell invasion in the castration resistant prostate cancer via targeting the androgen receptor splicing variant 7 (ARv7). *Cancer Lett.* **2017**, *398*, 62-69.
- (60) Shore, N. D. Darolutamide (ODM-201) for the treatment of prostate cancer. *Expert Opin. Pharmacother.* **2017**, *18* (9), 945-952.

Table 1. Initial biological evaluation of SARDs (class I)

ID	Our Initial Set of Compounds (Leading to Class I ^a AR Degraders)	Binding (K_i)/Transactivation (IC_{50}) (μ M)		SARD Activity (% degradation)	
		K_i (DHT = 1 nM) ^b	IC_{50} ^c	Full Length ^{d,e} (LNCaP) @ 1 μ M	Splice Variant ^{d,e} (22RV1) @ 10 μ M
1		0.032 ^{f, 27}	> 10	++	+
8		>10 ^{f, 27}	0.392	++	-
3		0.078 ^{g, 28}	0.048 ^{g, 28}	+++	+++

^a Class I is defined to be selective androgen receptor degraders in which the linker is a straight chain (e.g., butanamides or amino-propanamides). ^b AR binding was determined by competitive binding of 1 nM [³H]-mibolerone to recombinant ligand binding domain (LBD) of wildtype AR. DHT (1 nM) is used in each experiment as a standard agent. ^c Inhibition of transactivation was determined by transfecting HEK-293 cells with full length wildtype AR, GRE-LUC, and CMV-renilla luciferase for transfection control. And then 24 h later, treatment with 0.1 nM R1881 agonist and a dose response of antagonist (1 pM to 10 μ M in log units) for 24 h. Twenty four hours after treatment, cells were harvested and luciferase assay was performed using Dual Luciferase assay kit. ^d SARD activity was determined by treating LNCaP or 22RV1 cells, respectively, for determining FL AR or SV AR protein levels. Cells were maintained in charcoal-stripped serum-containing medium for 48 h and treated with the indicated doses of antagonist for 24 h in the presence of 0.1 nM R1881 (agonist). Cells were harvested and Western blot for AR was performed using AR-N20 antibody that is directed towards the N-terminal domain (NTD) of AR. The AR and AR SV bands were quantified and normalized to actin Western blots. ^e AR protein levels are reported qualitatively using the following abbreviations: -, no degradation (inactive); +, < 30% degradation (weak SARD activity); ++, 31 ~ 60% degradation (moderate SARD activity); +++, 61 ~ 90% degradation (strong SARD activity); +++++: > 90% degradation (complete SARD activity). ^f Binding data was determined as reported.²⁷ ^g We previously reported this binding and transactivation data in the same assays as reported here.²⁸

Table 2. Summary of structures of indolyl and indolinyl propanamides (Class II and III)

ID	Structure	ID	Structure	ID	Structure
7²⁸		18m		20a	
7r²⁸		18n		20b	
18a		18o		20e	
18b		18p		20f	
18c		18q		20g	
18e		19a		21a	
18f		19b		21b	
18g		19c		21c	
18i		19d		21d	
18j		19e		21e	
18k		19f		21f	
18l		19g		5	

Table 3. *In vitro* pharmacological activity of indolyl derivatives II

ID Class II ^a	Binding (K _i) / Transactivation (IC ₅₀) (μM)		SARD Activity (% degradation)	
	K _i (DHT = 1 nM) ^b	IC ₅₀ ^b	Full Length ^b (LNCaP)@1 μM	Splice Variant ^b (22RV1)@10 μM
7 (5-F)	0.267	0.085	+++	+++
7r (<i>R</i> -7)	>10.0	0.598	+++	+++
18a (unsub.)	2.080	0.064	+	++
18b (4-F)	0.419	0.127	++	++
18c (6-F)	0.212	0.085	-	+++
18e (5-NO ₂)	0.433	0.088	++	+++
18f (6-NO ₂)	0.047	0.058	-	+++
18g (3-Me, 5-F)	0.547	0.157	++	+++
II (3'-CF ₃) 18i (5-F, 6-Ph)	0.124	0.215	++	+
18j (5-Br)	0.316	0.918	-	-
18k (5-I)	0.294	0.985	-	+
18l (3-CO ₂ H)	>10.0	>10.0	-	-
18m (3-CO ₂ Et)	0.995	0.972	-	-
18n (4-pyridino, 5-CN)	>10.0	0.686	+	+
18o (4-Ph)	0.084	>10.0	-	-
18p (4-F, 5-Ph)	0.086	1.015	-	-
18q (4-F, 6-(4-F-Ph))	0.062	0.898	-	-
19a (3-F)	0.332	0.045	+++	+++
19b (4-F)	0.315	0.142	+++	++
19c (5-F)	0.253	0.094	+++	+
II (3'-Cl) 19d (6-F)	0.156	0.099	+++	-
19e (7-F)	0.720	0.234	++	+
19f (5-F, 6-Ph)	0.133	0.203	++	++
19g (3-Ph, 5-F)	0.135	1.032	-	-
2 [Enobosarm] ^c	0.0038	0.0038 ^c	Agonist ^d	Agonist ^d
4 [<i>R</i> -Bicalutamide]	0.509	0.248	-	-
5 [Enzalutamide]	3.641	0.216	-	-
6 [Apalutamide] ^e	1.452	0.016 ^e	+	-

^a Class **II** is defined to be selective androgen receptor degraders in which the B-ring is substituted or unsubstituted *N*-linked indole(i.e., indol-1-yl). ^b AR binding, transactivation, and degradation assays were performed and values reported as described in Table 1. ^c *In vitro* transcriptional activation was run in agonist mode and the EC₅₀ value was previously reported.³⁶ ^d Enobosarm is a full agonist that increases AR expression at the protein level. ^e *In vitro* transcriptional activation was run in antagonist mode and the IC₅₀ value was previously reported.⁵¹

Table 4. *In vitro* pharmacological activity of indolinyl derivatives III

ID Class III ^a	Binding (K_i) / Transactivation (IC_{50}) (μ M)		SARD Activity (% degradation)		
	K_i (DHT=1nM) ^b	IC_{50} ^b	Full Length (LNCaP)@1 μ M ^b	Splice Variant (22RV1)@10 μ M ^b	
III (3'-CF ₃)	20a (unsub.)	>1.0	0.142	+++	++
	20b (4-F)	0.170	0.059	+++	+
	20e (6-F)	0.273	0.039	+++	++
	20f (5,6-diF)	0.115	0.101 ^c	++	++
	20g (5-Cl, 6-F)	0.068	AG ^c	-	-
	21a (4-F)	0.382	0.126	++	+++
III (3'-Cl)	21b (5-F)	0.326	0.130	++	+
	21c (5-Br)	0.204	0.835	++	-
	21d (6-F)	0.490	0.037	++++	+
	21e (5,6-diF)	0.252	0.032	+++	++
	21f (5-F, 6-Ph)	0.071	0.244	++++	+++
	5	3.641	0.216	-	-

^a Class III is defined to be selective androgen receptor degraders in which the B-ring is substituted or unsubstituted *N*-linked indoline (i.e., indolin-1-yl). ^b AR binding, transactivation, and degradation assays were performed and values reported as described in Table 1. ^c AG, showed agonist activity.

Table 5. *In vitro* metabolic stability of II and III in mouse liver microsomes (MLM)

		MLM ^a				MLM ^a	
ID		T _{1/2} (min)	CL _{int} (mL/min/mg)	ID		T _{1/2} (min)	CL _{int} (mL/min/mg)
II (3'-CF ₃)	18 (5-F)	12.35	56.14	II (3'-Cl)	19a (3-F)	9.29	74.6
	18a (unsub.)	13.66	50.75		19b (4-F)	11.77	58.8
	18b (4-F)	36.32	19.08		19f (5-F, 6-Ph)	9.13	75.91
	18c (6-F)	22.39	30.96	III (3'-CF ₃)	20b (4-F)	25.06	27.67
	18e (5-NO ₂)	19.27	35.97		III (3'-Cl)	21a (4-F)	15.00
	18f (6-NO ₂)	13.48	51.43	21b (5-F)		9.16	23.77
	18g (3-Me, 5F)	21.77	31.84	21c (5-Br)		17.35	39.36
	18i (5F, 6Ph)	15.43	44.94	21f (5-F, 6-Ph)		21.37	32.44
	18j (5-Br)	17.02	40.73	21c (5-Br)		17.35	39.36
	18k (5-I)	20.37	34.02	Antagonist	5	10.04 ^b	86.3 ^c
18l (3-CO ₂ H)	29.79	23.28	Agonist	2	360.0	1.4	
18m (3-CO ₂ Et)	25.78	26.89					

^a Compounds are incubated together with MLM with co-factors for phase I and II provided, as described in the Experimental section. ^b T_{1/2} (h) after oral administration in humans as previously reported.⁵¹ ^c CL (mL/h/kg) after oral administration in humans as previously reported.⁵¹

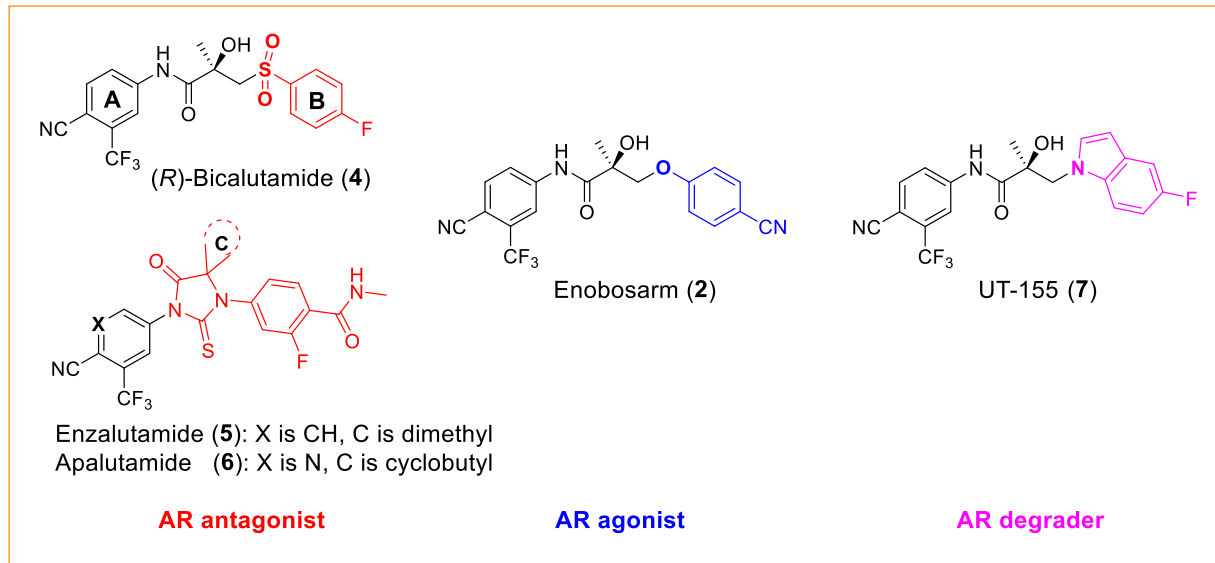


Figure 1. Known small molecule AR ligands: antagonists, agonist and degrader.

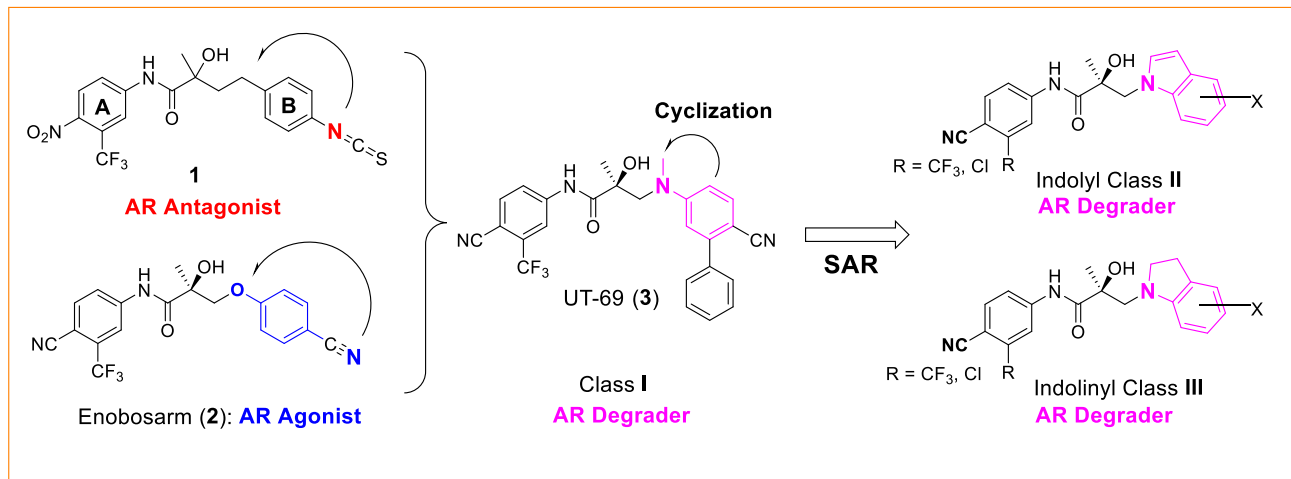


Figure 2. Design of diaryl indolyl and indolinyl propanamides (**II** and **III**) by structural modification of AR antagonists, e.g., **1**²⁷ and agonists, e.g., **2**³⁶ to produce several classes of AR degraders.

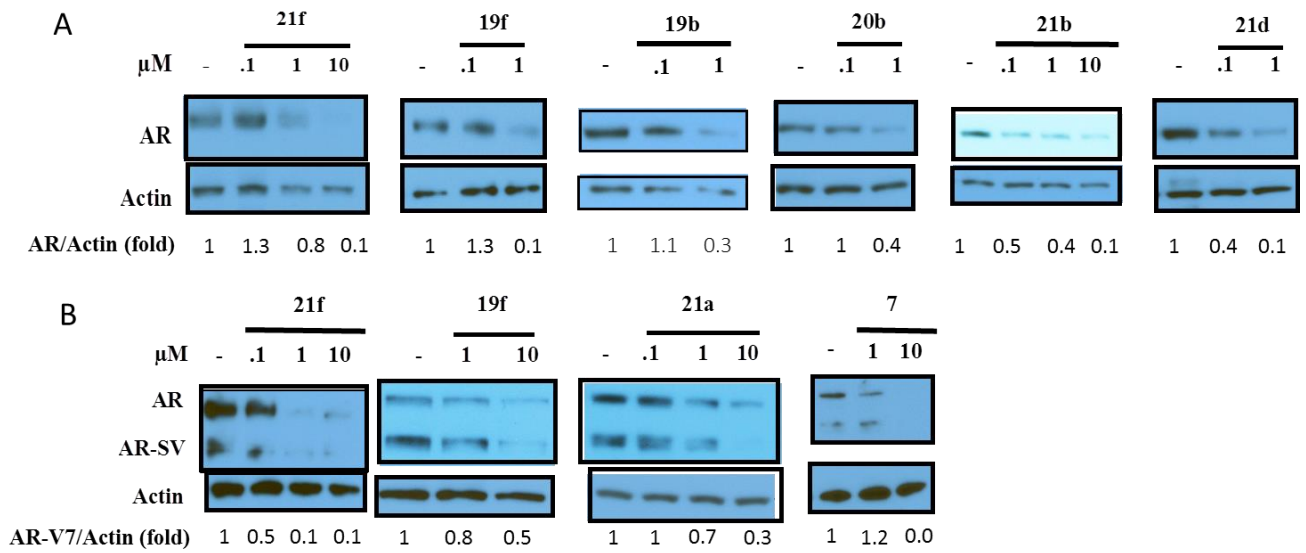
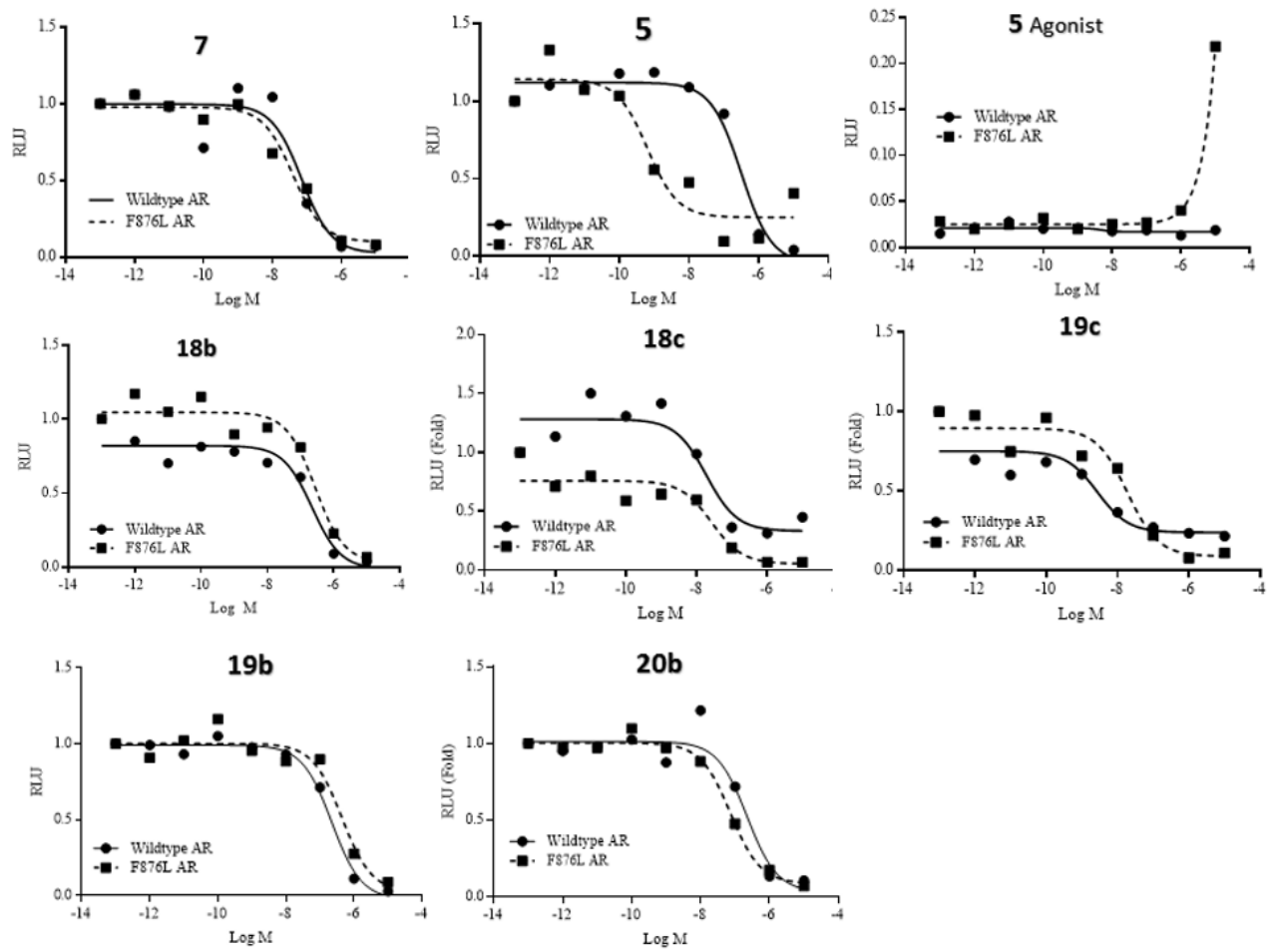


Figure 3: Degradation of FL and SV AR by selected SARDs. LNCaP (A) or 22RV1 (B) cells were plated in full-serum containing medium. Medium was changed to 1% charcoal-stripped serum containing medium and maintained in this medium for 2 days. Medium was changed again and the cells were treated with 0.1 nM R1881 (agonist) and either vehicle or a titration of SARD as indicated in the figure. Twenty-four hours after treatment, cells were harvested, protein extracted, and the proteins were blotted with AR-N20 antibody. Blots were stripped and re-probed with an actin antibody. The ratio of AR to actin for each lane is given under each blot. AR- full length androgen receptor; AR-SV- androgen receptor splice variant.

A



B

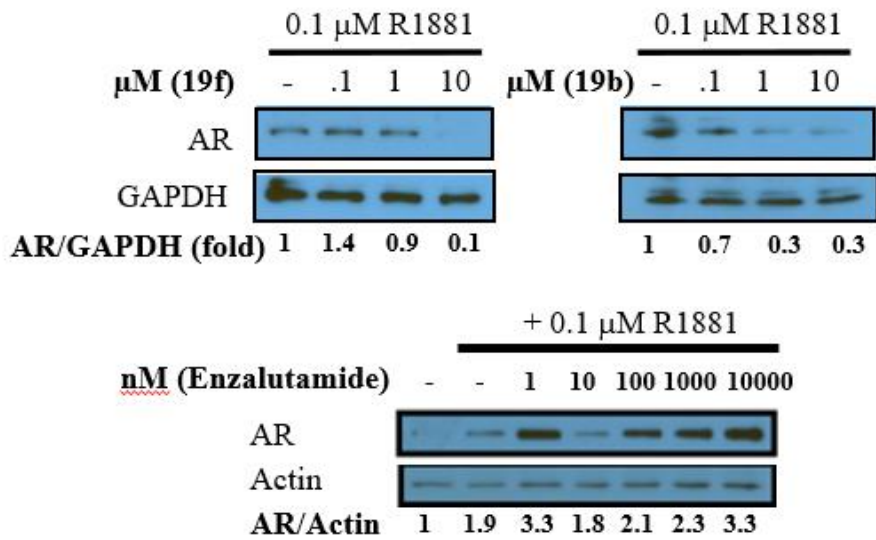


Figure 4: SARDs antagonize transactivation and degrade Enz-R conferring escape mutant AR. **A.** AR with phenylalanine 876 mutated to leucine (F876L), GRE-LUC, and CMV-renilla LUC were transfected in COS cells. Cells were treated 24 h after transfection with 0.1 nM R1881 (agonist) and a dose response of antagonists. Luciferase assay was performed 48 h after transfection. The effect of compound **5** was conducted in both antagonistic mode (in the presence of 0.1 nM R1881) and in agonistic mode (in the absence of 0.1 nM R1881). The agonist activity has been labeled in the figure as **5** (Agonist). **B.** Enzalutamide-resistant LNCaP cells (MR49F) were maintained in charcoal-stripped, serum containing medium for 2 d and treated with 0.1 nM R1881 (agonist) and a titration of the SARD or enzalutamide as indicated in the figure.

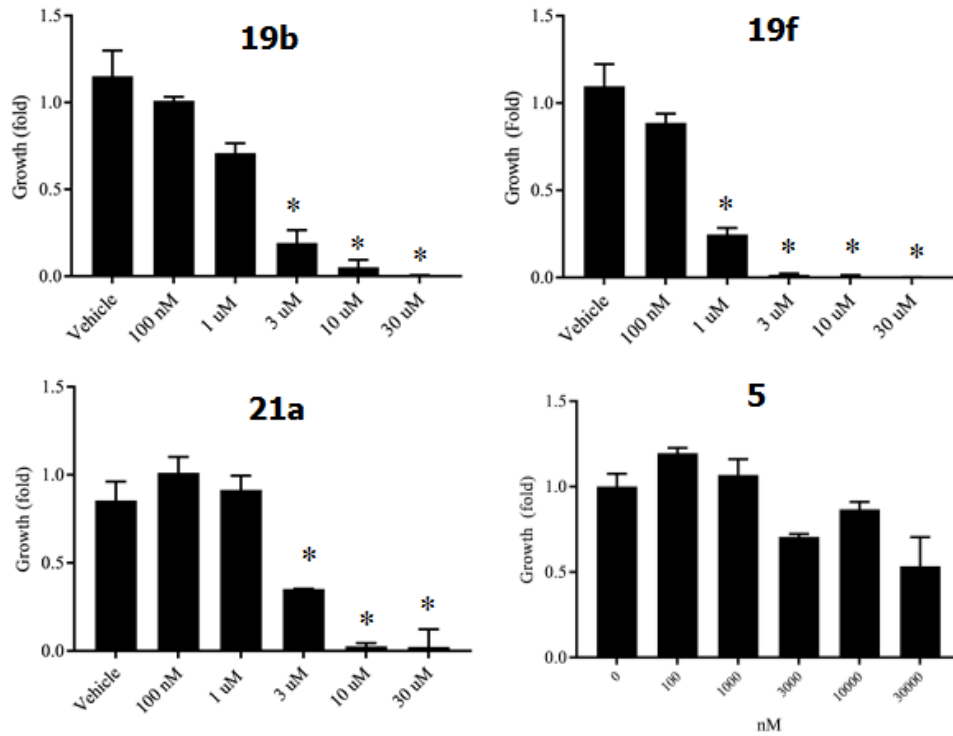
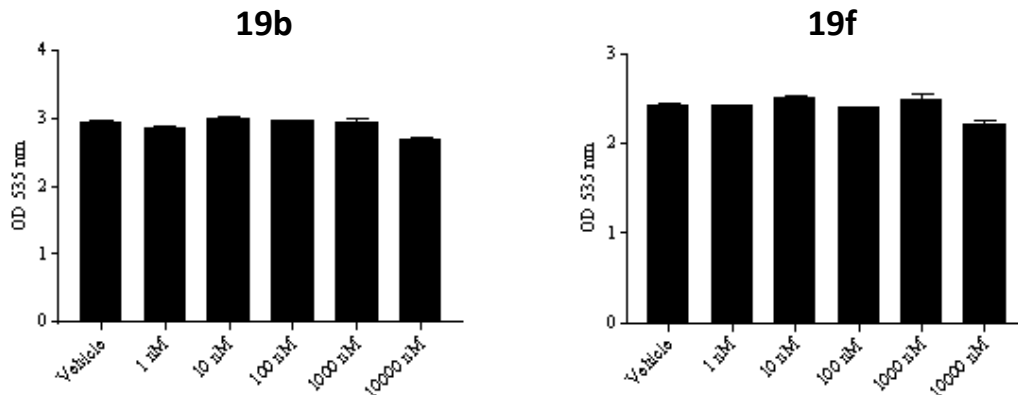
A**B**

Figure 5: Enzalutamide-Resistant LNCaP (MR49F) Cellular Anti-Proliferation: A. Enzalutamide-resistant LNCaP (MR49F) cells were plated in 1% charcoal-stripped, serum-containing medium and treated with 0.1 nM R1881 and titration of antagonist as indicated in the figure. Cells were re-treated 3 d after the first treatment and the number of viable cells measured by Cell-Titer Glo assay (Promega, Madison, WI). N = 3. * = $p < 0.05$. **B.** PC-3 cells were incubated with the indicated doses of the compounds in csFBS-containing medium. Medium was changed and the cells were re-treated after 3 days. Sulforhodamine B assay was performed after 6 days of treatment.

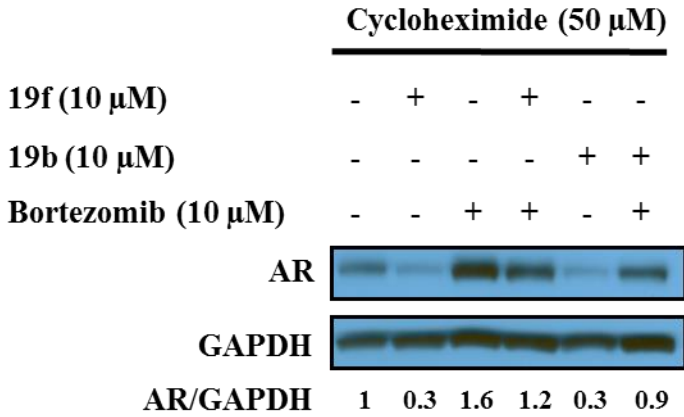
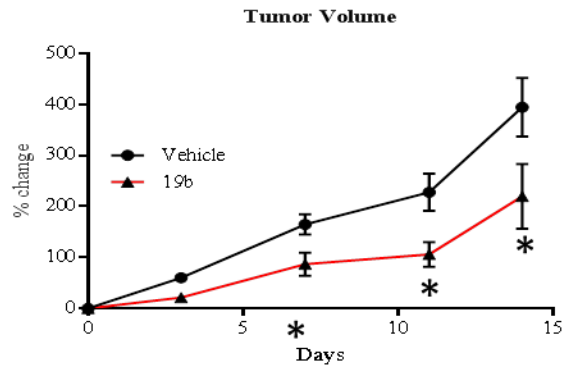
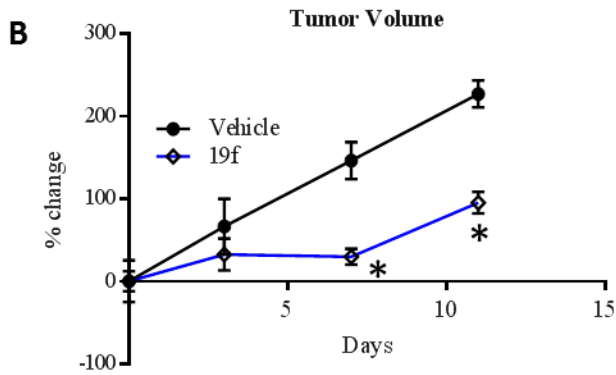
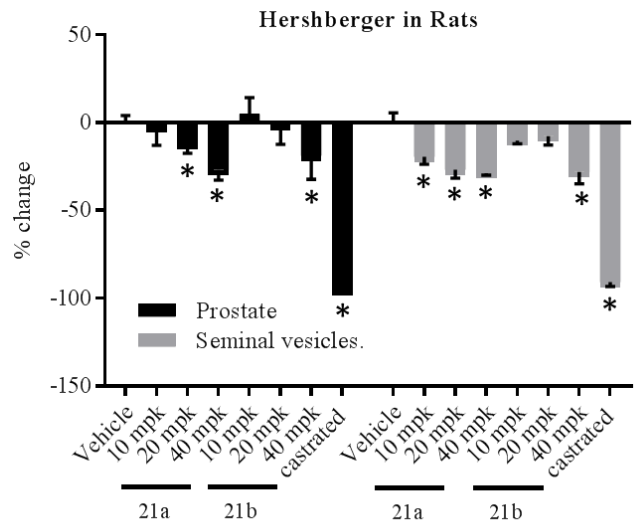
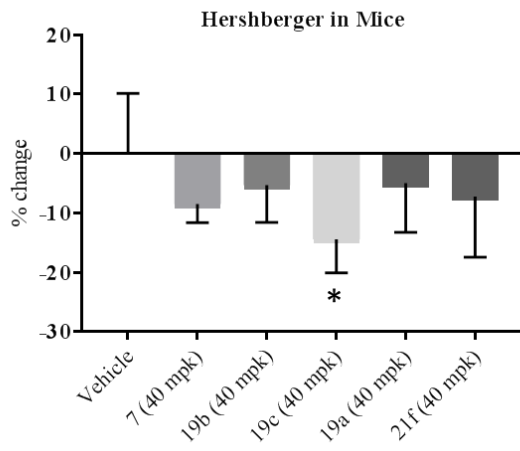
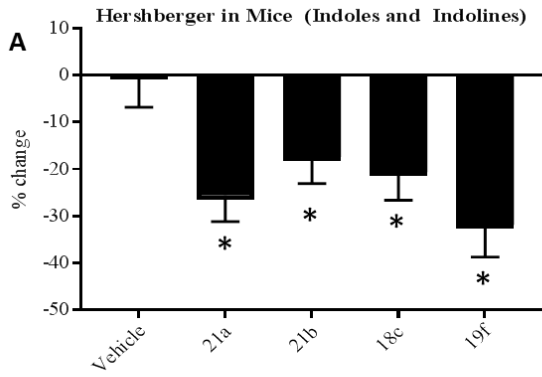


Figure 6: Proteasome inhibitor reverses the degradation of 19f and 19b in MR49F cells: LNCaP Enz-R cells (MR49F) were maintained in RPMI+10% FBS medium. Cells were treated in this medium for 8 hours. Cells were harvested, protein extracted, and Western blot for AR and GAPDH was performed. Quantification is provided at the bottom on the blots.



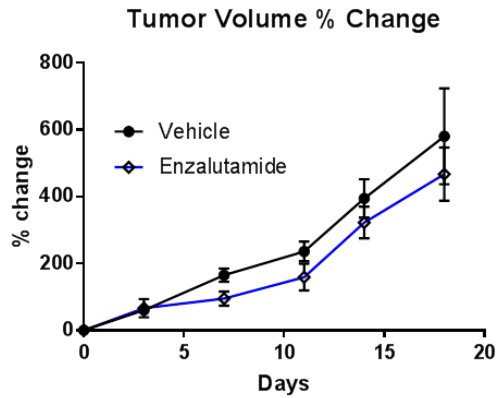
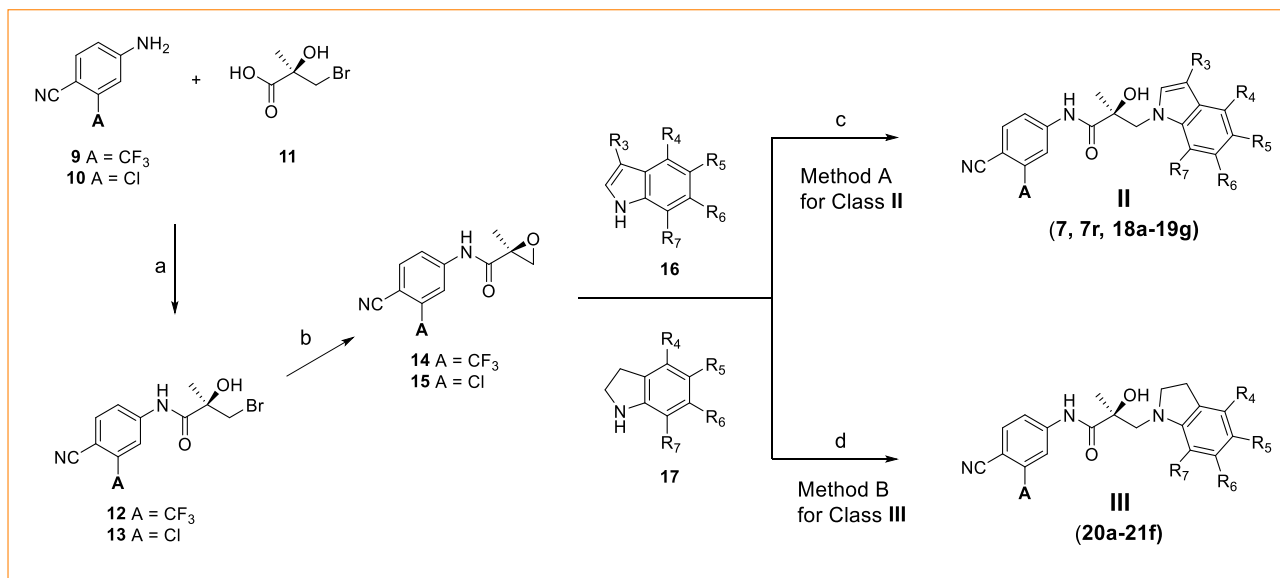


Figure 7: SARDs inhibit androgen-dependent organs in mice and rats and inhibit growth of enzalutamide-resistant prostate cancer. **A.** Mice (left) or rats (right) were treated with vehicle or indicated SARDs (40 mg/kg/day left panel) orally (n=5/group). Animals were sacrificed 14 d after treatment and weights of prostate and seminal vesicles were measured and normalized to body weight. **B.** Enzalutamide resistant LNCaP cells (5 million/mouse) were implanted subcutaneously in male NOD SCID Gamma (NSG) mice (n = 7-9 per group). Animals were castrated when the tumors reached 100-200 mm³ and allowed to regrow as castration-resistant tumors. Animals were treated orally with vehicle (DMSO:PEG-300 15:85) or 100 mg/kg/day of SARD or 30 mg/kg/day of enzalutamide. Tumor volume was measured twice weekly and represented as percent change. Values are expressed as average \pm S.E. *= p < 0.05.



Scheme 1. Generic synthesis of class **II** (compounds **7**, **7r**, **18a ~ 19g**) and **III** (compounds **20a ~ 21f**), Reagent and conditions: (a) SOCl₂, THF, 0 °C; (b) 2-butanone, K₂CO₃, reflux; (c) NaH, THF, 0 °C ~ room temperature; (d) LDA, THF, -78 °C ~ room temperature. * **7r** (*R*-isomer of **7**) was prepared from *L*-proline by same procedure as for **7**.

TABLE OF CONTENTS GRAPHIC (TOC)

